

23 **Abstract.** The structural framework provided by corals is crucial for reef ecosystem function and services, but high
24 seawater temperatures can be detrimental to the calcification capacity of reef-building organisms. The Red Sea is very
25 warm, but total alkalinity (TA) is naturally high and beneficial for reef accretion. To date, we know little about how
26 such beneficial and detrimental abiotic factors affect each other and the balance between calcification and erosion on
27 Red Sea coral reefs, that is overall reef growth, in this unique ocean basin. To provide estimates of present-day reef
28 growth dynamics in the central Red Sea, we measured two metrics of reef growth, i.e., *in situ* net-accretion/-erosion
29 rates (G_{net}) determined by deployment of limestone blocks and ecosystem scale carbonate budgets (G_{budget}) along a
30 cross-shelf gradient (25 km, encompassing near-, mid-, and offshore). Along this gradient, we assessed multiple
31 abiotic (i.e., temperature, salinity, diurnal pH fluctuation, inorganic nutrients, and TA) and biotic (i.e., calcifier and
32 epilithic bioeroder communities) variables. Both reef growth metrics revealed similar patterns from nearshore to
33 offshore: net-erosive, neutral, and net-accretion states. The average cross-shelf G_{budget} was $0.66 \text{ kg CaCO}_3 \text{ m}^{-2} \text{ y}^{-1}$, with
34 the highest budget of $2.44 \text{ kg CaCO}_3 \text{ m}^{-2} \text{ y}^{-1}$ measured in the offshore reef. These data are comparable to the
35 contemporary G_{budgets} from the western Atlantic and Indian Ocean, but lie well below "optimal reef production" (5 -
36 $10 \text{ kg CaCO}_3 \text{ m}^{-2} \text{ y}^{-1}$) and below maxima recently recorded in remote high coral cover reef sites. Yet, the erosive forces
37 observed in the Red Sea nearshore reef contributed less as observed elsewhere. A higher TA accompanied reef growth
38 across the shelf gradient, whereas stronger diurnal pH fluctuations were associated with negative budgets. Noteworthy
39 for this oligotrophic region was the positive effect of phosphate, which is a central micronutrient for reef building
40 corals. While parrotfish contributed substantially to bioerosion, our dataset also highlights coralline algae as important
41 local reef-builders. Altogether, our study establishes a baseline for reef growth in the central Red Sea that should be
42 useful in assessing trajectories of reef growth capacity under current and future ocean scenarios.

43

44 **1 Introduction**

45 Coral reef growth is mostly limited to warm, aragonite-saturated, and oligotrophic tropical oceans and is pivotal for
46 reef ecosystem functioning (Buddemeier, 1997; Kleypas et al., 1999). The coral reef framework not only maintains a
47 remarkable biodiversity, but also provides highly valuable ecosystem services that include food supply and coastal
48 protection, among others (Moberg and Folke, 1999; Reaka-Kudla, 1997). Biogenic calcification, erosion, and
49 dissolution contribute to the formation of the reef framework constructed of calcium carbonate (CaCO_3 , mainly
50 aragonite). The balance of carbonate loss and accretion is influenced by biotic and abiotic factors. On a reef scale, the
51 main antagonists are calcifying benthic communities on the one hand, such as scleractinian corals and coralline algal
52 crusts, and grazing and endolithic bioeroders on the other hand, such as parrotfish, sea urchins, microbioeroding
53 chlorophytes, boring sponges, and other macroborers (Glynn, 1997; Hutchings, 1986; Perry et al., 2008; Tribollet and
54 Golubic, 2011). The export or loss of carbonate as sediments is considered an essential part, in particular in the wider
55 geomorphic perspective of reef carbonate production states (Cyronak et al., 2013; Perry et al., 2008, 2017).
56 Temperature and carbonate chemistry parameters (e.g., pH, total alkalinity: TA, and aragonite saturation state: Ω_a ,
57 $p\text{CO}_2$) have been identified as important players in regulating these carbonate accretion and erosion processes
58 (Albright et al., 2018; Schönberg et al., 2017). Furthermore, different light regimes across depths, water flow, and
59 wave exposure can alter the rates of reef-formation processes (Dullo et al., 1995; Glynn and Manzello, 2015; Kleypas
60 et al., 2001).

61
62 Reef growth is maintained when reef calcification produces more CaCO_3 than is being removed, and depends largely
63 on the ability of benthic calcifiers to precipitate calcium carbonate from seawater (e.g., Langdon et al., 2000; Tambutté
64 et al., 2011). TA and Ω_a positively correlate with calcification rates (Marubini et al., 2008; Schneider and Erez, 2006),
65 and while calcification rates of corals and coralline algae increase with higher temperature, they have upper thermal
66 limits (Jokiel and Coles, 1990; Marshall and Clode, 2004; Vásquez-Elizondo and Enríquez, 2016). Today's Oceans
67 are warming and high temperatures begin to exceed the thermal optima of calcifying organisms and thereby slowing
68 down or interrupting calcification (e.g., Carricart-Ganivet et al., 2012; Death et al., 2009). At the same time, ocean
69 acidification decreases the Oceans' pH and Ω_a (Orr et al., 2005). Arguably, calcification under these conditions
70 becomes energetically costlier (Cai et al., 2016; Cohen and Holcomb, 2009; Strahl et al., 2015; Waldbusser et al.,
71 2016). In addition, ocean acidification stimulates destructive processes, for instance the proliferation of bioeroding
72 endolithic organisms (e.g., Enochs, 2015; Fang et al., 2013; Tribollet et al., 2009). Apart from that, locally impaired
73 reef growth due to an increased intensity or frequency of extreme climate events (Eakin, 2001; Schuhmacher et al.,
74 2005), human impacts including pollution and eutrophication (Chazottes et al., 2002; Edinger et al., 2000), and other
75 ecological events such as population outbreaks of grazing sea urchins or crown-of-thorn starfish that feed on coral can
76 induce reef framework degradation (Bak, 1994; Pisapia et al., 2016; Uthicke et al., 2015).

77
78 A number of studies have employed experimental limestone blocks cut from coral skeletons to study reef growth
79 processes (Chazottes et al., 1995; Kiene and Hutchings, 1994; Silbiger et al., 2014; Tribollet and Golubic, 2005).
80 Deployment of such blocks in a reef captures the endolithic and epilithic accretion and erosion agents and forces,

81 simultaneously allowing for the measurement of net-accretion and net-erosion rates. In particular, these studies have
82 provided insight into the colonization progression and activity of endolithic micro- and macroorganisms. To
83 comparatively assess the persistence of reef framework at the ecosystem scale, a census-based reef carbonate budget
84 (*ReefBudget*) approach that integrates reef site-specific ecological data into the calculation of the erosion-accretion
85 balance was introduced recently (Kennedy et al., 2013; Perry et al., 2012, 2015). Using the *ReefBudget* approach, a
86 recent study determined that 37 % of all current reefs that were investigated are in a net-erosive state (Perry et al.,
87 2013). For the Caribbean, it revealed a 50 % decrease of reef growth compared to historical mid- to late-Holocene
88 reef growth (Perry et al., 2013). Indeed, the use of carbonate budgets provided valuable insight into the reef growth
89 trajectories in the Seychelles, where surveys conducted since the 1990s provide important ecological baseline data
90 that were employed in reef growth calculations (Januchowski-Hartley et al., 2017). Most recently, carbonate budget
91 data were used to explore the relation of vertical reef growth potential and trends in sea level rise suggesting that reef
92 submergence poses a threat as long as climate-driven and human-made perturbations persist (Perry et al., 2018). Other
93 studies highlight the susceptibility of marginal coral reefs to ocean warming and acidification (Couce et al., 2012).
94 Such marginal reefs are found in the Eastern Pacific or in the Middle East in the Persian/Arabian Gulf, where reefs
95 exist at their environmental limits, e.g., at low pH or high temperatures, respectively (Bates et al., 2010; Manzello,
96 2010; Riegl, 2003; Sheppard and Loughland, 2002).

97
98 Although the Red Sea features high sea surface temperatures that exceed thermal thresholds of tropical corals
99 elsewhere (Kleypas et al., 1999; Osman et al., 2018), it supports a remarkable coral reef framework along its entire
100 coastline (Riegl et al., 2012). Yet, coral skeleton core samples indicate that calcification rates have been declining
101 over the past decades, which has been widely attributed to ocean warming (Cantin et al., 2010). In this regard Red
102 Sea coral reefs are on a similar trajectory as other coral reefs under global ocean warming (Bak et al., 2009; Cooper
103 et al., 2008). In the central and southern Red Sea, present-day data show reduced calcification rates of corals and
104 calcifying crusts when temperatures peak during summer (Roik et al., 2015; Sawall et al., 2015). While increasing
105 temperatures are seemingly stressful and energetically demanding for reef calcifiers, high TA values, as found in the
106 Red Sea (~ 2400 $\mu\text{mol kg}^{-1}$, Metzl et al. 1989), are indicative of a putatively beneficial environment for calcification
107 (Albright et al., 2016; Langdon et al., 2000; Tambutté et al., 2011). At present, little is known about the reef-scale
108 carbonate budgets of Red Sea coral reefs (Jones et al., 2015). Apart from one early assessment of reef growth capacity
109 for a high-latitude reef in the Gulf of Aqaba (GoA, northern Red Sea) that considered both calcification and
110 bioerosion/dissolution rates (Dullo et al., 1996), studies only report calcification rates (e.g., Cantin et al., 2010; Heiss,
111 1995; Roik et al., 2015; Sawall and Al-Sofyani, 2015) or focus on bioerosion generally caused by one group of
112 bioeroders (Alwany et al., 2009; Kleemann, 2001; Mokady et al., 1996). Therefore, we set out to determine reef growth
113 in central Red Sea coral reefs and evaluate the biotic and abiotic drivers. We show and compare two reef growth
114 metrics: G_{net} and G_{budget} . We present net-accretion/-erosion rates (G_{net}) measured *in situ* using limestone blocks
115 deployed in the reefs, which simultaneously capture the rates of epilithic accretion and epilithic and endolithic
116 bioerosion. We also apply a census-based approach adapted from the *ReefBudget* protocol (Perry et al., 2012) to
117 estimate reef growth on an ecosystem scale, as the net carbonate production state or carbonate budget (G_{budget}). Our

118 study provides a broad and first insight into reef growth dynamics and a comparative baseline to further assess the
119 effects of environmental change on reef growth in the central Red Sea.
120

121 2 Material and Methods

122 2.1 Study sites and environmental monitoring

123 Study sites are located in the Saudi Arabian central Red Sea along an environmental cross-shelf gradient, described in
124 detail in Roik et al. (2015) and Roik et al. (2016). Data for this study were collected at three sites: an offshore forereef
125 at ~25 km distance from the coastline (22° 20.456 N, 38° 51.127 E, “Shi’b Nazar”), midshore forereef at ~10 km
126 distance (22° 15.100 N, 38° 57.386 E, “Al Fahal”), and a nearshore forereef (22° 13.974 N, 39° 01.760 E, “Inner
127 Fsar”) at ~3 km distance to shore. All sampling stations were located between 7.5 and 9 m depth. In the following,
128 reef sites are referred to as “offshore”, “midshore”, and “nearshore”, respectively. Abiotic variables were measured
129 during “winter” and “summer” 2014. CTD data was collected continuously during “winter” (9th February - 7th April
130 2014) and “summer” (19th June - 23th October 2014). At each station, seawater samples were collected on SCUBA for
131 5 - 6 consecutive weeks during each of the seasons to determine inorganic nutrients, i.e., nitrate and nitrite (NO₃⁻
132 & NO₂⁻), ammonia (NH₄⁺), phosphate (PO₄³⁻), and total alkalinity (TA) (Table S1).

133

134 2.2 Net-accretion/-erosion rates of limestone blocks

135 Net-accretion/-erosion rates (G_{net}) were assessed using a “limestone block assay”. Blocks cut from “coral stone”
136 limestone were purchased from a local building material supplier in Jeddah, KSA. Each block was fixed with one
137 stainless steel bolt to aluminum racks permanently deployed at the monitoring station of each reef site (a total of 36
138 blocks, $n = 4$, Fig. S1). The blocks were oriented in parallel to the reef slope with one side facing up while the other
139 side was facing down towards the reef. Block dimensions were 100 x 100 x 21 mm with an average density of $\rho = 2.3$
140 kg L⁻¹. Blocks were dry-weighed before and after deployment on the reefs (Mettler Toledo XS2002S, readability = 10
141 mg). Before weighing, the blocks were autoclaved and dried in a climate chamber (BINDER, Tuttlingen, Germany)
142 at 40 °C for a week. Four replicate blocks were deployed at the reef sites for three different exposure periods each
143 (Fig. 1 a) to measure natural processes of calcification and erosion. Exposure periods were 6 months (September 2012
144 - March 2013), 12 months (June 2013 - June 2014), and 30 months each (January 2013-June 2015). We measured a
145 total of 12 blocks and all blocks were measured only once. Upon recovery, the blocks were treated with 10 % bleach
146 for 24 - 36 h and rinsed with deionized water to remove organic material and any residual salts. G_{net} were expressed
147 as normalized differences of pre-deployment and post-deployment weights [kg CaCO₃ m⁻² y⁻¹] (Table 1).

148

149 2.3 Biotic parameters

150 To assess coral reef benthic calcifier and epilithic bioeroder communities (as input data for the reef carbonate budgets),
151 we conducted *in situ* surveys on SCUBA along the cross-shelf gradient at each of our study sites.

152

153 2.3.1 Benthic community composition

154 Community composition and coverage of coral reef calcifying groups were assessed in six replicate transects per site
155 using the belt-transect rugosity method (Perry et al., 2012) as detailed in Roik et al. (2015). From these surveys we
156 extracted data on benthic calcifiers (% cover total hard coral, % hard coral morphs (branching, encrusting, massive,
157 and platy/foliose), % major reef-building coral families (Acroporidae, Pocilloporidae, and Poritidae), % cover
158 calcareous crusts, % recently dead coral, and % rock surface area for carbonate budget calculations (Table S2). In
159 addition, benthic rugosity was assessed in the same transects following the *Chain and Tape Method* (n = 6, Perry et
160 al., 2012).

161

162 2.3.2 Epilithic bioeroder/grazer populations along the cross-shelf gradient

163 For each reef site, we surveyed abundances and size classes of the two main groups of coral reef framework epilithic
164 bioeroders, parrotfishes (Scaridae) (Bellwood, 1995; Bruggemann et al., 1996) and sea urchins (Echinoidea) (Bak,
165 1994). Surveys were conducted on SCUBA using stationary plots (adapted from Bannerot and Bohnsack, 1986, Text
166 S1) and line transects (n = 6 per site), respectively. Briefly, abundances of parrotfishes and sea urchins were assessed
167 for different size classes. Abundances for all prevalent parrotfish species were assessed in six size classes, based on
168 estimated fork length (FL; FL size classes: 1 = 5 - 14 cm, 2 = 15 - 24 cm, 3 = 25 - 34 cm, 4 = 35 - 44 cm, 5 = 45 - 70,
169 and 6 > 70 cm). We focused on the most abundant bioeroding parrotfish species in the Red Sea (Table S4), which
170 encompassed two herbivorous functional groups: excavators and scrapers (Green and Bellwood 2009). Most abundant
171 across study sites were the excavators *Chlorurus gibbus*, *Scarus ghobban*, and *Cetoscarus bicolor*, and the scrapers
172 *Scarus frenatus*, *Chlorurus sordidus*, *Scarus niger* and *Scarus ferrugineus*, following Alwany et al., 2009.
173 Additionally, we counted *Hipposcarus harid*, which occurred frequently at the study sites, along with members of the
174 genus *Scarus* that could not be identified to species level and were therefore pooled in the category ‘Other *Scarus*’.
175 Both *H. harid* and *Scarus* spp. were broadly categorized as scrapers (Green and Bellwood, 2009). The sea urchin
176 census targeted five size classes of the four most common bioerosive genera *Diadema*, *Echinometra*, *Echinostrephus*,
177 and *Eucidaris*, based on urchin diameter (size classes 1 = 0 - 20 mm, 2 = 21 - 40 mm, 3 = 41 - 60 mm, 4 = 61 - 80
178 mm, 5 = 81 - 100 mm, Table S7). For details on the field surveys and data treatment for biomass conversion, refer to
179 the supplementary materials (Text S1 and references therein).

180

181 2.4 Reef carbonate budgets

182 Ecosystem scale reef carbonate budgets, G_{budget} [kg CaCO₃ m⁻¹ y⁻¹], were determined following the census-based
183 *ReefBudget* approach by Perry et al. (2012) (Table 1). G_{budget} incorporates local census data, site-specific net-
184 accretion/-erosion data (G_{net} over 30 months) and calcification data (buoyant weight measurements) collected for this
185 and a previous study (Roik et al., 2015). Importantly, the approach incorporates epilithic bioerosion, which is based
186 on abundance rather than bite or erosion rates; therefore, parrotfish and sea urchin census data collected in this study
187 were employed in the *ReefBudget* calculations using bite and erosion rates from the literature (Alwany et al., 2009;

188 Perry et al., 2012). In summary, site-specific benthic calcification rates (G_{benthos} , $\text{kg CaCO}_3 \text{ m}^{-1} \text{ y}^{-1}$), net-accretion/
189 erosion rates of reef “rock” surface area ($G_{\text{netbenthos}}$, $\text{kg CaCO}_3 \text{ m}^{-1} \text{ y}^{-1}$), and epilithic erosion rates by sea urchins (E_{echino} ,
190 $\text{kg CaCO}_3 \text{ m}^{-1} \text{ y}^{-1}$) and parrotfishes (E_{parrot} , $\text{kg CaCO}_3 \text{ m}^{-1} \text{ y}^{-1}$), were determined for the G_{budget} calculations (Fig. 1 (b)
191 and Fig. 3 (a)). A detailed account of Red Sea specific calculations and modifications of the *ReefBudget* approach
192 employed in this study are outlined in the supplementary materials (Text S1, Equation box S1-3, and Tables S2-S8).

193

194 **2.5 Abiotic parameters**

195 **2.5.1 Continuous data: temperature, salinity, and diurnal pH variation**

196 Factory-calibrated conductivity-temperature-depth loggers (CTDs, SBE 16plusV2 SEACAT, RS-232, Sea-Bird
197 Electronics, Bellevue, WA, USA) were deployed at the monitoring stations on tripods at ~0.5 m above the reef to
198 collect time series data of temperature, salinity, and pH_{NBS} at hourly intervals. The pH probes (SBE 18/27, Sea-bird
199 Electronics) were factory calibrated before the winter deployment (9th February - 7th April 2014). Calibrations were
200 verified using NBS scale standard buffers (pH 7 and 10, Fixanal, Fluka Analytics, Sigma Aldrich, Germany) before
201 the winter and the summer deployment (19th June - 23th October 2014).

202

203 **2.5.2. Seawater samples: Inorganic nutrients and total alkalinity**

204 Seawater samples were collected on SCUBA at each of the stations using 4 L collection containers (Table S1).
205 Simultaneously, 60 mL seawater samples were taken through a 0.45 μm syringe filter for TA measurements. Seawater
206 samples for inorganic nutrient analyses and TA measurements were transported on ice in the dark and were processed
207 on the same day. Samples were filtered over GF/F filters (0.7 μm , Whatman, UK) and filtrates were frozen at -20°C
208 until analysis. The inorganic nutrient content (NO_3^- & NO_2^- , NH_4^+ , and PO_4^{3-}) was determined using standard
209 colorimetric tests and a Quick-Chem 8000 AutoAnalyzer (Zellweger Analysis, Inc.). TA samples were analyzed
210 within 2 - 4 h after collection using an automated acidimetric titration system (Titrand 888, Metrohm AG,
211 Switzerland). Gran-type titrations were performed with a 0.01 M HCl (prepared from 0.1 M HCl Standard, Fluka
212 Analytics) at an average accuracy of $\pm 9 \mu\text{mol kg}^{-1}$ (standard deviation of triplicate measurements).

213 **2.6 Statistical analyses**

214 **2.6.1 Net-accretion/-erosion rates and carbonate budgets**

215 G_{net} data (Table 2) were tested for effects of the factors “reef” (fixed factor: nearshore, midshore, and offshore) and
216 “deployment time” (random factor: 6, 12, and 30 months). A univariate 2-factorial PERMANOVA was performed on
217 $\log_n(x)$ transformed data (i.e., $\log_n(x+1-\min(x_{1-n}))$) as data contained negative and near-zero values). A Euclidian
218 distance matrix and 9999 permutations of residuals under a reduced model and type III partial sum of squares were
219 employed. Pair-wise tests followed where applicable (PRIMER-E V6, Table S9).

220 G_{budget} data (Table 3) were tested for statistical differences between the reef sites (fixed factor: nearshore, midshore,
221 and offshore) using a 1-factorial ANOVA. In parallel, G_{benthos} was tested using a 1-factorial ANOVA with \log_{10}

222 transformed data, while non-parametric Kruskal-Wallis tests were employed for non-transformed $G_{\text{netbenthos}}$, E_{echino} ,
223 and E_{parrot} data. Tukey's HSD post-hoc tests or Dunn's multiple comparisons followed where applicable (Table S10).
224 Assumptions about parametric distribution of data were evaluated using the Shapiro-Wilk normality test. Statistical
225 tests were performed as implemented in R (R Core Team, 2013).

226

227 **2.6.2 Abiotic parameters**

228 All abiotic data were summarized as means and standard deviations per reef and season and over each season (Table
229 4) and boxplots were generated (Fig. 4). Diurnal pH variation was extracted from the continuous data as the pH_{NBS}
230 standard deviation per day. Outliers were detected and removed from the TA data. All outliers (data points beyond
231 the upper boxplot 1.5 IQR) clustered to one sampling day (23 June 2014), which we considered an artifact of the
232 chemical analysis and the outliers from this day were removed. All continuous abiotic variables and inorganic nutrients
233 (PO_4^{3-} after square-root transformation) fulfilled parametric assumptions and were evaluated using univariate 2-
234 factorial ANOVAs testing the factors "reef" (nearshore, midshore, and offshore) and "season" (winter and summer).
235 TA data was square-root transformed, which improved symmetry of data (Anderson et al., 2008), and tested under the
236 same 2-factorial design, as outlined above, using a PERMANOVA (Euclidian resemblance matrix and 9999
237 permutations of residuals under a reduced model and type II partial sums of squares). Within each significant factor,
238 Tukey's HSD post-hoc tests or PERMANOVA integrated pair-wise tests followed (Table S11 and S12). Assumptions
239 were evaluated by histograms and the Shapiro-Wilk normality test. Statistical tests and outlier detection were
240 performed in R or PRIMER-E V6.

241

242 **2.6.3 Abiotic-biotic correlations**

243 To evaluate the relationship of abiotic and biotic predictors of G_{net} and G_{budget} , Spearman rank correlation coefficients
244 were obtained for the predictor variables (at a confidence level of 95%) using *cor.test* in R (R Core Team, 2013;
245 Wickham and Chang, 2015). *P*-values were adjusted using *p.adjust* in R employing the Benjamini-Hochberg method.
246 Correlations were performed using G_{net} data obtained in the 30-months measurements from the reef sites (nearshore,
247 midshore, and offshore) (Table 5 and Table S13). Predictor variables were the site-specific means of CTD measured
248 variables (temperature, salinity, and diurnal pH variation), means of inorganic nutrients (NO_3^- & NO_2^- , NH_4^+ , and PO_4^{3-}
249), and TA (Table 4). Biotic predictors were variables that likely impacted the limestone blocks, i.e. parrotfish
250 abundances, sea urchin abundances, calcareous crusts cover, and algal and sponge cover. Since we did not observe
251 any coral recruits of substantial size on the blocks, we did not include % coral cover and related variables in the
252 correlations.

253 G_{budget} correlations included all the above-mentioned abiotic variables and 13 biotic transect variables (i.e., parrot fish
254 abundances, sea urchin abundances, % branching coral, % encrusting coral, % massive coral, % platy/foliose coral,
255 % of Acroporidae, % Pocilloporidae, % Poritidae, % total hard coral cover, calcareous crusts cover, algal and sponge

256 cover, and rugosity). Prior to analysis, some of the predictors (i.e., % platy/foliose corals and % Poritidae) were
257 $\log_{10}(x+1)$ transformed to improve the symmetry in their distributions (Table 5 and Table S14).
258

259 **3 Results**

260 **3.1 Net-accretion/-erosion rates of limestone blocks**

261 Net-accretion/-erosion rates G_{net} were measured in assays over periods of 6, 12, and 30 months in the reef sites along
262 the cross-shelf gradient. These measurements represent the result of calcification and bioerosion processes impacting
263 the deployed limestone blocks. Visible traces of boring endolithic fauna were only found on the surface of blocks
264 recovered after 12 and 30 months as presented in Fig. 2 (c)-(f). A brief visual inspection of the block surfaces after
265 retrieval showed colonization by coralline algae, bryozoans, boring sponges, small size boring worms and clams, as
266 well as parrotfish bite-marks. **No coral recruits were noticed by the unaided eye.** Further analyses of the established
267 presence of calcifying and bioeroding communities were not within the scope of this study. G_{net} based on the 30-
268 months deployment of blocks ranged between -0.96 and $0.37 \text{ kg CaCO}_3 \text{ m}^{-2} \text{ y}^{-1}$ (Table 2). G_{net} for 12 and 30-months
269 blocks were negative on the nearshore reef (between -0.96 and $-0.6 \text{ kg CaCO}_3 \text{ m}^{-2} \text{ y}^{-1}$, i.e., net erosion is apparent),
270 slightly positive on the midshore reef ($0.01 - 0.06 \text{ kg CaCO}_3 \text{ m}^{-2} \text{ y}^{-1}$, i.e., almost neutral carbonate production state),
271 and positive on the offshore reef (up to $0.37 \text{ kg CaCO}_3 \text{ m}^{-2} \text{ y}^{-1}$, i.e., net accretion of reef framework). Deployment
272 times had a significant effect on the variability of G_{net} (Pseudo- $F = 5.9$, $p_{\text{PERMANOVA}} < 0.01$, Table S9). As expected,
273 accretion/erosion was overall higher when measured over the longer deployment period (Fig. 2 (g)) in comparison to
274 the shorter deployment times, reflecting the continuous and exponential nature of bioerosion due to the colonization
275 progress of fouling organisms over time. The significant interaction of reef site and deployment time (Pseudo- $F = 7.3$,
276 $p_{\text{PERMANOVA}} < 0.001$) shows that only blocks deployed over 12 and 30 months revealed significant site variability,
277 specifically the differences between nearshore vs. offshore and midshore vs. offshore sites became evident ($p_{\text{pair-wise}} <$
278 0.05 , Table S9). The within-group variability was highest for the nearshore reef, where standard deviations were up
279 to 7-times higher compared to the midshore and the offshore reefs.

280

281 **3.2 Biotic parameters**

282 **3.2.1 Benthic community composition**

283 A detailed account of benthic community structure of the study sites is provided in Roik et al. (2015). In brief, a low
284 percentage of live substrate (20 %) and calcifier community cover (hard corals = 11 % and calcifying crusts = 1 %) were
285 characteristic for the nearshore site, while rock (23 %) and rubble (4 %) were more abundant compared to the
286 other sites. The midshore and offshore reefs provided live benthos cover of around 70 % and a large proportion of
287 calcifiers (48 and 59 %). The proportion of coral and calcifying crusts, which were dominated by coralline algae, were
288 38 % and 10 % in the midshore reef compared to 35 % and 23 % in the offshore reef, respectively. Major reef-building
289 coral families were Acroporidae, Pocilloporidae, and Poritidae forming 32 - 56 % of the total hard coral cover. A soft
290 coral community (of around 25 %) occupied large areas in the midshore reef. This community was minor in the
291 nearshore and offshore reefs with 4 % and 8.5 %, respectively. Specific benthic accretion rates G_{benthos} [$\text{kg CaCO}_3 \text{ m}^{-2} \text{ y}^{-1}$],
292 which were used as input data for the G_{budget} calculation, were determined using these benthic data in addition
293 to site and calcifier specific calcification rates (Tables S2 and S3).

294

295 **3.2.2 Epilithic bioeroder/grazer populations along the cross-shelf gradient**

296 A total of 718 parrotfishes and 110 sea urchins were observed and included in subsequent *ReefBudget* analyses.
297 Parrotfish mean abundances and biomass estimates ranged between 0.08 ± 0.01 and 0.17 ± 0.60 individuals m^{-2} , and
298 24.69 ± 6.04 and 82.18 ± 46.67 g m^{-2} , respectively (Table S4). The largest parrotfish (category 5 parrotfish, i.e., > 45
299 - 70 cm fork length) were observed at the midshore site. With the exception of the midshore reef, category 1 (5 - 14
300 cm) parrotfish were commonly observed at all sites. Large parrotfish (category 6 with > 70 cm fork length) were not
301 observed during the surveys. For sea urchins, mean abundances of 0.002 ± 0.004 - 0.014 ± 0.006 individuals m^{-2} per
302 site were observed and mean biomasses 0.05 ± 0.04 - 1.43 ± 0.98 g m^{-2} estimated per site, respectively (Table S7).
303 The midshore site exhibited the largest range of sea urchin size classes (from categories 1 or 2 to the largest size class
304 5), while at the other two exposed sites, only the two smallest size classes of sea urchins were recorded.

305

306 **3.3 Reef carbonate budgets**

307 The carbonate budget, G_{budget} , averaged over all sites was 0.66 ± 2.01 kg CaCO_3 m^{-2} y^{-1} encompassing values ranging
308 from a negative nearshore budget (-1.48 ± 1.75 kg CaCO_3 m^{-2} y^{-1}) to a positive offshore budget (2.44 ± 1.03 kg CaCO_3
309 m^{-2} y^{-1}) (Figure 3 and Table 3). G_{budget} significantly differed between reef sites ($F = 16.7$, $p_{\text{ANOVA}} < 0.001$, Table S10),
310 where nearshore vs. offshore site and midshore vs. offshore site showed significant differences ($p_{\text{Tukey HSD}} < 0.01$).
311 Further, biotic variables that contribute to the final G_{budget} were diverse: G_{benthos} significantly varied between midshore
312 vs. nearshore site and offshore vs. nearshore site ($p_{\text{Tukey HSD}} < 0.01$), $G_{\text{netbenthos}}$ varied between all site combinations
313 ($p_{\text{Tukey HSD}} < 0.001$), E_{echino} significantly differed between midshore and nearshore, and E_{parrot} variability was similar at
314 all sites. The within-group variation for the nearshore reef was 5-times higher compared to the midshore reef and the
315 offshore reef. Overall, the proportional loss of accreted carbonate to bioerosion was 15 % in the offshore reef, 42 %
316 in the midshore reef, and the loss even exceeded the accretion by four-fold in the nearshore reef, i.e., ~ 440 %
317 proportional loss when considering accreted carbonate to bioerosion.

318

319 **3.4 Abiotic parameters**

320 **3.4.1 Temperature, salinity, and diurnal pH variation**

321 We used abiotic monitoring data to characterize environmental conditions at each reef site throughout the year (Table
322 1, Table S11 and S12). Temperature and salinity comprised ~4400 data points per reef site in the nearshore and
323 offshore reef, and ~2700 in the midshore reef; diurnal pH standard deviations comprised 185 data points for the
324 midshore and offshore site, and 87 for the nearshore site. The seasonal mean temperature varied between 26.1 ± 0.5
325 °C in winter and 30.9 ± 0.7 °C in summer across all reefs. The cross-shelf difference was largest in summer (~0.6 °C),
326 and significant during both seasons ($F = 1042.6$, $p_{\text{ANOVA}} < 0.001$). From all sites, the nearshore site experienced the

327 lowest mean temperature (26.1 °C) in winter and the highest (31.3 °C) in summer. In comparison, the midshore and
328 offshore reefs were slightly cooler with means around 30.6 °C during summer. Overall salinity was high ranging
329 between 39.18 – 39.44 over the year. In summer nearshore salinity was significantly increased by 0.36 compared to
330 winter and by 0.18 compared to the other reefs ($F = 945.3, p_{ANOVA} < 0.001$). Salinity in the midshore and offshore reef
331 was not significantly different between the two sites. Mean diurnal standard deviations of pH ranged between 0.04 –
332 0.07 of pH units in the midshore and offshore reefs. The nearshore reef experienced the largest diurnal variations as
333 indicated by mean diurnal standard deviations of 0.29 pH units during winter and 0.6 pH units during summer. The
334 diurnal pH fluctuation differed significantly between all reef sites ($F = 1241, p_{ANOVA} < 0.001$).

335

336 3.4.2 Seawater samples: Inorganic nutrients and total alkalinity

337 Concentrations of all measured inorganic nutrients were below 1 $\mu\text{mol kg}^{-1}$ (Table 1). NO_3^- & NO_2^- was on average
338 between 0.63 ± 0.26 and $0.28 \pm 0.22 \mu\text{mol kg}^{-1}$, NH_4^+ between 0.51 ± 0.17 and $0.35 \pm 0.19 \mu\text{mol kg}^{-1}$, and PO_4^{3-} as low
339 as 0.02 ± 0.01 and $0.09 \pm 0.02 \mu\text{mol kg}^{-1}$ (the highest and lowest site-season averages are reported here). By trend,
340 mean NO_3^- & NO_2^- and NH_4^+ levels were higher in winter compared to summer with a difference of 0.29 and 0.16 μmol
341 kg^{-1} , respectively (Fig. 4, Table S11 and S12). In contrast, PO_4^{3-} was significantly higher in winter than in summer
342 with means differing on average by 0.04 $\mu\text{mol kg}^{-1}$ ($F = 16, p_{ANOVA} < 0.001$, Table S11). Mean differences across the
343 shelf were 0.1 $\mu\text{mol kg}^{-1}$ in NO_3^- & NO_2^- during winter, 0.1 $\mu\text{mol kg}^{-1}$ in NH_4^+ during summer, and 0.02 $\mu\text{mol kg}^{-1}$ in
344 PO_4^{3-} throughout both seasons. TA ranged between 2391 ± 15 and $2494 \pm 16 \mu\text{mol kg}^{-1}$. TA was significantly different
345 between seasons and reef sites (Pseudo- $F_{\text{season}} = 297.6$, Pseudo- $F_{\text{reefsite}} = 22.5$, $p_{\text{PERMANOVA}} < 0.001$, Table S11 and
346 S12). During both seasons, TA was decreasing from the offshore to the nearshore reef. During winter, TA was slightly
347 higher with $2487 \pm 20 \mu\text{mol kg}^{-1}$ compared to $2417 \pm 27 \mu\text{mol kg}^{-1}$ during summer. The increase from nearshore to
348 offshore was on average between 20 and 50 $\mu\text{mol kg}^{-1}$ (Fig. 4).

349 3.5 Abiotic-biotic correlations

350 To explore the relationship between environmental variables and reef growth, we performed correlation analyses. For
351 G_{net} , strong, positive, and significant correlates were calcareous crust cover, NO_3^- & NO_2^- , PO_4^{3-} , and TA. Negative
352 correlates were salinity, diurnal pH variation, and parrotfish abundance (strong correlates: $\rho > |0.75|$, $p < 0.001$). For
353 G_{budget} , abiotic correlates were NO_3^- & NO_2^- , PO_4^{3-} , and TA, the same correlates as for G_{net} . Looking at significant biotic
354 correlates of G_{budget} , we only found positive relationships, including calcareous crusts, hard corals, and rugosity.
355 Conversely, parrotfish and sea urchin abundances had a negative effect on G_{budget} , but the correlation was weak and
356 not significant ($\rho \sim -0.5$). The non-calcifying benthos, which represents the coverage by algae, soft corals, and sponges,
357 was not correlated with the dynamics of G_{budget} and was correlated only weakly and not significantly with G_{net} ($\rho \sim$
358 0.5) (Table 5, Tables S13 and S14).

359

360 **4 Discussion**

361 Central Red Sea reefs are characterized by unique environmental conditions of high temperature, salinity, TA, and
362 oligotrophy (Fahmy, 2003; Kleypas et al., 1999; Steiner et al., 2014). On a global scale they support remarkable reef
363 growth, supporting well established fringing reefs along most of the coastline. To date, processes affecting reef growth
364 in various regions of the Red Sea have mostly been investigated individually. For instance, some studies focused on
365 bioerosion by one specific group of bioeroders only (Alwany et al., 2009; Kleemann, 2001; Mokady et al., 1996),
366 while other studies assessed calcification of reef-building corals (e.g., Cantin et al., 2010; Heiss, 1995; Roik et al.,
367 2015; Sawall et al., 2015). To provide a more comprehensive picture, the present study integrated assessment of the
368 antagonistic processes of calcification and bioerosion. We achieved this in a two-step approach assessing two central
369 metrics of reef growth along a cross-shelf gradient. First, we assessed net-accretion/-erosion rates (G_{net}) from three
370 reef sites along the cross-shelf gradient *in situ* using a limestone block assay. Second, we constructed ecosystem-scale
371 estimates of reef carbonate budgets for Red Sea reef sites (G_{budget}) adapting the census-based *ReefBudget* approach by
372 Perry et al. (2012). In the following, we highlight the complex dynamics and interactions of reef growth processes and
373 discuss the importance of carbonate budgets as a powerful tool to explore the trajectories of reef growth in a global
374 and historical context.

375

376 **4.1 Net-accretion/-erosion rates (G_{net}) in the central Red Sea**

377 **4.1.1 Cross-shelf dynamics in a global context**

378 The limestone block assay revealed three reef production states in the central Red Sea: 1) net erosion (nearshore), 2)
379 near-neutrality (midshore), and 3) net accretion (offshore). This is in contrast to the pattern observed on the Great
380 barrier reef (GBR), where total bioerosion rates were higher in offshore reefs than inshore reefs as assessed from
381 limestone blocks (Tribollet et al., 2002; Tribollet and Golubic, 2005). Generally, most block assay studies conducted
382 in various reef habitats and regions found net-erosive rates. For instance, studies from reefs in the Thai Andaman Sea
383 and Indonesian Java Sea note that the accretion by calcifying crusts, such as coralline algae, were negligible compared
384 to the high degree of bioerosion measured in the limestone blocks (Edinger et al., 2000; Schmidt and Richter, 2013).
385 In contrast, our limestone block assays captured a substantial net accretion rate, in particular for the offshore reef site
386 in the central Red Sea ($0.37 \text{ kg CaCO}_3 \text{ m}^{-2} \text{ y}^{-1}$ net accretion), indicating that accretion was substantial, while erosion
387 was negligible. The midshore reef was characterized by a near-neutral or minor net accretion ($0.06 \text{ kg CaCO}_3 \text{ m}^{-2} \text{ y}^{-1}$)
388 on the order of net accretion rates recorded in French Polynesia in reef sites of uninhabited, oceanic atolls (0.08 and
389 $0.62 \text{ kg CaCO}_3 \text{ m}^{-2} \text{ y}^{-1}$; Pari et al., 1998). Notably, our study recorded a net-erosive state only in the Red Sea nearshore
390 site ($-0.96 \text{ kg CaCO}_3 \text{ m}^{-2} \text{ y}^{-1}$, 30 months deployment). This is a moderate rate compared to the larger net erosion
391 observed in the GBR, French Polynesia, and Thailand (-4 or $-8 \text{ kg CaCO}_3 \text{ m}^{-2} \text{ y}^{-1}$) (Osorno et al., 2005; Pari et al.,
392 1998; Schmidt and Richter, 2013; Tribollet and Golubic, 2005).

393

394

395 4.1.2 Limestone block deployment duration and biotic drivers

396 Our data show that G_{net} values were overall higher with longer deployment times, reflecting the succession and early
397 establishment of calcifying crust and bioeroding communities on the limestone blocks. Due to our sampling design
398 (weight-based block assay), accretion and erosion processes however are simultaneously captured and cannot be
399 disentangled. Overall, the block assay data are indicative of a calcifier-beneficial offshore environment and a nearshore
400 reef habitat that is supporting endolithic bioeroders.

401 Following other work, carbonate loss in the 12-month blocks from the nearshore site was supposedly due to a young
402 microbioeroder community, which is typically most active during this early phase. For instance, during the early stages
403 of colonization by endolithic microorganisms, the chlorophyte *Ostreobium* sp. predominantly contributes to
404 microbioerosion, while the erosion rate steadily increases with deployment time (Grange et al., 2015; Tribollet and
405 Golubic, 2011). Microbioerosion rates have been reported to be $-0.93 \text{ kg CaCO}_3 \text{ m}^{-2} \text{ y}^{-1}$ after 12 months of block
406 exposure, which represents the average rate at the early colonization stage when the steadily increasing
407 microbioerosion rate has leveled off (Grange et al., 2015). This rate is slightly higher compared to our measurements
408 of net erosion in the nearshore site after the same deployment time (i.e. $-0.61 \text{ kg CaCO}_3 \text{ m}^{-2} \text{ y}^{-1}$), and the difference
409 may reflect measurements encompassing both, bioerosion and accretion.

410 Studies have shown that site differences in total bioerosion are typically becoming visible after 1 year of deployment
411 and are significantly enhanced after 3 years (Tribollet and Golubic, 2005). In line with this, the deployment time of
412 12 months in our study was sufficient to reveal differences between the nearshore and offshore reef sites. Further,
413 calcifying crusts, specifically coralline algae, observed on all blocks from the offshore reef contributed to the
414 respective net accretion. This is corroborated by the positive correlation of their abundances with G_{net} across all reef
415 sites. **Given that we could not identify coral recruits on any limestone block, we assume that contribution of corals to**
416 **the measured accretion was minor. However, we acknowledge that we might have missed some that could be detected**
417 **by more sophisticated methods (e.g. such as microscopic examination).**

418 Significant differences in accretion/erosion between all three sites of the cross-shelf gradient became apparent after
419 30 months deployment, and macroborer traces were observed in blocks for the first time (Fig. 2). Over the course of
420 2 - 3 years, macrobioeroders such as polychaetes, sipunculids, bivalves, and boring sponges can establish communities
421 in limestone blocks (Hutchings, 1986). Between the first two years, macrobioeroder contribution to the total bioerosion
422 can quadruple ($0.02 - 0.09 \text{ kg CaCO}_3 \text{ m}^{-2} \text{ y}^{-1}$), before levelling off around 3 - 4 years post-deployment (Chazottes et
423 al., 1995).

424 In our study, the increase of G_{net} between the 12- and 30-month deployment ($\sim 0.30 \text{ kg CaCO}_3 \text{ m}^{-2} \text{ y}^{-1}$ on average in
425 the nearshore and offshore site) indicates that calcifying and eroding communities were still in a state of succession.
426 As such, we cannot unequivocally rule out that the blocks deployed for 30 months still represented an immature
427 community, and hence, underestimated maximal calcification and erosion rates.

428 Correlation analyses indicate a significant contribution of parrotfish to the net erosion rates in the nearshore reef. This
429 observation is in line with previous work demonstrating a significant contribution of parrotfish activity to bioerosion
430 (Alwany et al., 2009; Bellwood, 1995; Bellwood et al., 2003). By comparison, sea urchin size and abundance do not
431 appear to be significant for bioerosion on the central Red Sea reefs. On other reefs, sea urchin bioerosion can be

432 substantial, equaling or even exceeding reef carbonate production (Bak, 1994). The low contribution of sea urchins to
433 bioerosion on central Red Sea reefs may be a result of potentially low abundances of highly erosive sea urchins
434 (McClanahan and Shafir, 1990). This is in line with the observed parrotfish bite-marks and a lack of sea urchins on
435 and in the direct vicinity of the recovered blocks. Taken together, our data confirms that endolithic micro- and
436 macrobioerosion, as well as parrotfish feeding, likely provides a substantial contribution to calcium carbonate loss.
437

438 4.2 Carbonate budgets (G_{budget}) in the central Red Sea

439 4.2.1 Cross-shelf dynamics, regional and global context

440 On an ecosystem scale, the G_{budget} data suggest that the offshore reef site in the central Red Sea loses about 15 %
441 accreted carbonates to bioerosion per year. On the mid- and nearshore reef this loss increases to to 42 % and to over
442 100 %, respectively. By comparison, on the scale of a single coral colony, the boring clam *Lithophaga lessepsiana*
443 alone can erode up to 40 % of the carbonate deposited by the coral *Stylophora pistillata* (Lazar and Loya, 1991). In
444 our study sites, the spatial dynamics of the two metrics G_{net} and the census-based G_{budget} , were consistent and suggest
445 net erosion in nearshore reef sites and net accretion in offshore reef sites in the central Red Sea. Reef growth at the
446 central Red Sea cross-shelf gradient averaged $0.66 \pm 2.01 \text{ kg CaCO}_3 \text{ m}^{-2} \text{ y}^{-1}$, which was driven by the substantial
447 budget of the offshore reef, reflecting the location and habitat dependence for reef growth potential. That the offshore
448 reef budget is essential to maintain the entire shelf budget has also been observed on a reef platform in the
449 Maldives. In the respective study, reef accretion was minor and highly heterogeneous at most sites and only few reef
450 sites at the platform margin promoted substantial net accretion and thereby greatly contributed to the positive average
451 budget of the entire platform (Perry et al., 2017).

452 The here presented central Red Sea G_{budget} data are within the range of contemporary reef carbonate budgets from the
453 Atlantic ($2.55 \pm 3.83 \text{ kg CaCO}_3 \text{ m}^{-2} \text{ y}^{-1}$) and Indian Ocean ($1.41 \pm 3.02 \text{ kg CaCO}_3 \text{ m}^{-2} \text{ y}^{-1}$) (Perry et al., 2018). Notably,
454 these data are below the suggested “optimal reef budget” of 5 - 10 $\text{kg CaCO}_3 \text{ m}^{-2} \text{ y}^{-1}$ observed in “healthy”, high coral
455 cover fore-reefs (see data in Perry et al., 2018 and comparisons therein; Vecsei, 2001, 2004). The decline in coral
456 cover is likely central to the reduced carbonate budgets in contemporary reefs. For instance, the reefs investigated in
457 the present study do not exceed a coral cover of 40 % (as observed in the offshore study site). In comparison, the
458 dataset compiled by Vecsei 2001 encompasses hard coral cover of up to 80% for the Indo-Pacific and up to 95 % for
459 Pacific Islands. Further, the reduced contemporary carbonate budgets coincide with the observed decrease in
460 calcification rates of Red Sea corals at large (Cantin et al., 2010; Steiner et al., 2018). As such, the effect of climate
461 change and the corresponding increase in seawater temperature may have severe consequences via overall decrease
462 in coral reef cover as well as via reduced calcification of the resident corals. Hence, although the present G_{budget} data
463 still suggest effective barrier reef formation in the central Red Sea (substantial accretion on the offshore reef),
464 carbonate accretion rates and therefore reef formation in the central Red Sea may be hampered in the long run by the
465 ongoing warming.
466

467 **4.2.2 Biotic drivers**

468 *Regional differences*

469 Cross-shelf patterns of G_{budget} drivers from the central Red Sea are distinct from other reef systems. The central Red
470 Sea system is characterized by a nearshore site with a negative G_{budget} , impacted by high parrotfish abundances and
471 erosion rates, low coral cover, and putatively considerable endolithic bioerosion rates (see discussion of G_{net} data).
472 Conversely, the offshore reef is characterized by high calcification rates, driven by high coral and coralline algae
473 abundances. In the GBR an opposing trend with high net accretion in the nearshore reefs (Browne et al., 2013)
474 coincided with high coral cover, low bioerosion rates, and lowest rates of parrotfish bioerosion (Hoey and Bellwood,
475 2007; Tribollet et al., 2002). On Caribbean reefs, parrotfish erosion rates were higher on leeward reefs (which may be
476 similar to protected nearshore habitats), but in contrast to the central Red Sea, these sites were typically characterized
477 by overall high coral cover driving a positive G_{budget} (Perry et al., 2012, 2014). This inter-regional comparison strongly
478 suggests that reef accretion/erosion dynamics encountered in any given reef system cannot be readily extrapolated to
479 other reef systems. Hence, *in situ* assessments of individual reef systems are required to unravel local dynamics and
480 responses to environmental change, and are therefore imperative for the development of effective management
481 measures.

482

483 *The role of coral and coralline crusts*

484 Benthic calcifiers, in particular reef-building corals, are major contributors to carbonate production and are considered
485 the most influential drivers of G_{budgets} globally (Franco et al., 2016). Corals in particular can contribute as much as 90
486 % to the gross carbonate production across different reef zones, which also includes low coral cover lagoonal and
487 rubble habitats (Perry et al., 2017). Hence, loss of coral cover rapidly gives way to increased bioerosion and thereby
488 critically contributes to reef framework degradation (Perry and Morgan, 2017). Indeed, on Caribbean reefs, G_{budget}
489 data were reported to shift into erosional states once live hard coral cover was below 10 % (Perry et al., 2013). A live
490 coral cover threshold remains to be determined for the central Red Sea and will require evaluation of a larger dataset.
491 Yet, we find that the nearshore reef featuring a negative G_{budget} is characterized by a coral cover of 11 %, while the
492 midshore and offshore reefs, characterized by near-neutral vs. positive carbonate budgets, both feature similar average
493 coral covers (at 35 and 40 %, respectively). In this respect, our data show that a 2-fold higher abundance of coralline
494 algae and other encrusting calcifiers in the offshore reef (compared to the midshore reef) significantly added to a
495 higher G_{budget} . The positive contribution of coralline algae for central Red Sea reef accretion is corroborated by their
496 strong and significant correlation to G_{budget} . Coralline algae in particular are considered an important contributor to
497 reef growth, as they stabilize the reef framework through “cementation” (Perry et al., 2008) and by habitat priming
498 for successful coral recruitment (Heyward and Negri, 1999).

499

500 *Epilithic grazers*

501 Epilithic grazers such as parrotfish and sea urchin are considered important drivers of bioerosion on many reefs (Hoey
502 and Bellwood, 2007; Mokady et al., 1996; Pari et al., 1998; Reaka-Kudla et al., 1996). Sea urchins were identified as
503 significant bioeroders in some reefs of Réunion Island, French Polynesia, and in the GoA, northern Red Sea (Chazottes

504 et al., 1995, 2002; Mokady et al., 1996). For the northern Red Sea, sea urchins were abundant, and their removal of
505 reef carbonates was estimated to range around 13 - 22 % of total reef slope calcification (Mokady et al., 1996). In
506 contrast, sea urchins were rare in our study sites contributing to only 2 - 3 % of the total bioerosion resulting in low
507 contributions to G_{budget} . Only on the net-erosive nearshore reef were sea urchins more abundant causing 12 % of total
508 bioerosion.

509 Compared to sea urchins, parrotfish played a more important role for G_{budgets} throughout the entire reef system,
510 contributing 70 - 96 % of the total bioerosion. In the correlation analyses, both grazers, i.e., sea urchins and parrotfish,
511 negatively correlated with G_{budget} , however these correlations were not very strong ($\rho \sim -0.5$) and non-significant. The
512 weak correlation may be influenced by a considerable variability in the reef census dataset, specifically regarding
513 parrotfish abundances. Observer bias (parrotfish keep minimum distance from surveyors during dives and may
514 therefore not enter survey plots; pers. obs.), natural (e.g., species distribution, habitat preferences, reef rugosity, and
515 mobility or large roving excavating species, such as *Bolbometopon muricatum*), and/or anthropogenically-driven
516 factors (e.g., differential fishing pressure) may also contribute to the observed data heterogeneity (McClanahan, 1994;
517 McClanahan et al., 1994). Indeed, the Saudi Arabian central Red Sea has been subject to decade-long fishing pressure,
518 which has significantly altered reef fish community structures and reduced overall fish biomass compared to less
519 impacted Red Sea regions (Kattan et al., 2017). Unregulated fishing could at least in part explain the differences of
520 fish abundance dynamics between the present study and reefs on the GBR and the Caribbean. **The heterogeneity of**
521 **grazer populations further propagates into G_{budgets} estimates, resulting in a considerable within-site variability that**
522 **reduces power of statistical tests and correlations.**

523 **4.3 Abiotic factors and reef growth dynamics**

524 Reef habitats in the central Red Sea are characterized by abiotic factors that differ from the majority of tropical reef
525 environments (Couce et al., 2012; Kleypas et al., 1999). Our sites were exposed to high summer temperatures (30 -
526 33 °C) and a high salinity throughout the year (39 - 40). Inorganic nutrients were mostly far below 1 $\mu\text{mol kg}^{-1}$,
527 whereas TA was comparably high, 2400 – 2500 $\mu\text{mol kg}^{-1}$, values typical for much of the Red Sea basin (Acker et al.,
528 2008; Steiner et al., 2014). As such, the Red Sea is considered a natural model system or “laboratory”, which can
529 advance our understanding of ecosystem functioning under extreme or marginal conditions of which some are
530 projected under ocean change scenarios (Camp et al., 2018). The study of such natural systems is a challenge and the
531 documentation of governing factors both abiotic and biotic will contribute to a better understanding of the dynamics
532 and interactions, which can significantly improve ecosystem scale predictions (Boyd and Hutchins, 2012; Boyd and
533 Brown, 2015; Camp et al., 2018). In the present study, reef framework decline (i.e., net erosion) was associated with
534 the reef habitat of slightly increased salinity and stronger diel pH fluctuations, which are characteristic for shallow
535 water, limited flow systems and semi-enclosed reefs (Camp et al., 2017; Shamberger et al., 2017), such as the here
536 investigated nearshore study site (Roik et al., 2016). On the other hand, positive reef growth was associated with reef
537 habitats characterized by higher TA levels, but also with slightly increased inorganic nutrient species, namely NO_3^-
538 & NO_2^- and PO_4^{3-} .

539

540 *The nearshore site*

541 The nearshore reef is located on the shelf, surrounded by shallow waters of extended residency time and has a lower
542 water exchange rate compared to the other two reef sites (Roik et al., 2016). Evaporation and limited flow, particularly
543 during summer, may increase salinity, which was overall higher at this reef site. However, the difference to the other
544 sites was minuscule and unlikely to have affected calcifying (Röthig et al., 2016) and bioeroding biota. The variability
545 of diurnal pH on the other hand presumably has stronger impacts on the performance of calcifiers and bioeroders.
546 Previously, pH variability across a reef flat and slope were demonstrated to correlate with net accretion dynamics by
547 showing higher net accretion prevailing in sites of less variable pH conditions (Price et al., 2012; Silbiger et al., 2014),
548 which reflects the pattern observe here.

549 The fluctuation in pH may (in part) represent a biotic feedback signature in reef habitats, which entails changes in sea
550 water chemistry caused by dominant biotic processes, i.e., calcification, carbonate dissolution, and
551 respiration/photosynthesis (Bates et al., 2010; Silverman et al., 2007a; Zundeleovich et al., 2007). Commonly, such pH
552 fluctuations are influenced by changes in carbonate system variables, e.g. DIC and TA (Shaw et al., 2012; Silbiger et
553 al., 2014), which can modify the antagonistic processes of calcification and bioerosion/dissolution (e.g., Andersson,
554 2015; Langdon et al., 2000; Tribollet et al., 2009). In particular, in our nearshore study site, where benthic macro
555 community abundance was low, biological activity in the sandy bottom (e.g., permeable carbonate sands) might be a
556 crucial factor contributing to the biotic feedback (Andersson, 2015; Cyronak et al., 2013; Eyre et al., 2018).

557

558 *Total alkalinity and nutrients*

559 The increase in TA is often associated with increased carbonate ion concentration and Ω_a , which facilitate the
560 precipitation of carbonates supporting the performance of reef-builders (Albright et al., 2016, 2018; Langdon et al.,
561 2000; Schneider and Erez, 2006; Silbiger et al., 2014). We identified a positive correlation of TA with reef growth in
562 our dataset. The difference in TA across our study sites was small, but in the range of natural cross-shelf differences
563 reported from other reefs (e.g. reefs in Bermuda, 20 - 40 $\mu\text{mol kg}^{-1}$, Bates et al., 2010), and as high as 50 $\mu\text{mol kg}^{-1}$,
564 the TA enrichment that enhanced community net calcification in a reef-enclosed lagoon (Albright et al., 2016). On
565 the other hand, high calcification rates can deplete TA, whereas dissolution of carbonates can enrich TA measurably,
566 specifically in (semi) enclosed systems (Bates et al., 2010), which we do not observe along the cross shelf gradient. It
567 remains to be further investigated how TA dynamics across the shelf relate to reef growth processes.

568 Although increased nutrients are commonly linked to reef degradation initiated through phase shifts, increased
569 bioerosion rates, and/or the decline of calcifiers (Fabricius, 2011; Grand and Fabricius, 2010; Holmes, 2000), our
570 dataset suggests that a highly oligotrophic system such as the central Red Sea reefs may benefit from slight increases
571 of certain nutrient species. Specifically, natural minor increases of N and P might have a positive effect on ecosystem
572 productivity and functioning including carbonate budgets. A moderate natural source of nutrients, e.g., from sea bird
573 populations, can indeed have a positive effect on ecosystem functioning, in contrast to anthropogenic run-off (Graham
574 et al., 2018). Interestingly, our study also identified PO_4^{3-} concentration as an abiotic correlate of reef growth. In the
575 Red Sea, high N:P ratios indicate that P is a limiting micronutrient, e.g. for phytoplankton (Fahmy, 2003). PO_4^{3-} is not
576 only essential for pelagic primary producers, but also for reef calcifiers and their photosymbionts, such as the stony

577 corals and their micro-algal Symbiodiniaceae endosymbionts (Ferrier-Pagès et al., 2016; LaJeunesse et al., 2018).
578 Experimental studies have demonstrated that PO_4^{3-} provision can maintain the coral-algae symbiosis in reef-building
579 corals under heat stress (Ezzat et al., 2016). Conversely, P limitation can increase the stress susceptibility of this
580 symbiosis (Pogoreutz et al., 2017; Rådecker et al., 2015; Wiedenmann et al., 2013). In light of our results, it will be
581 of interest to link spatio-temporal variation of inorganic nutrient ratios with patterns of reef resilience in the central
582 Red Sea to understand their effects on long-term trends of reef growth.

583

584 **4.4 Reef growth trajectories in the Red Sea**

585 Carbonate budgets provide an insight into ecosystem functioning and can be used as a powerful tool to track reef
586 trajectories through time. This includes the exploration of past and current reef trends, which may be critical for
587 prediction of future reef development (Januchowski-Hartley et al., 2017). Indeed, the absence of comparative baseline
588 data limits a historical perspective on the central Red Sea G_{budget} presented here. Previously reported Red Sea data
589 include pelagic and reefal carbonate accretion rates from 1998, estimated using basin-scale historical measurements
590 of TA (Steiner et al., 2014). Another dataset employed the census-based budget approach for a highly seasonal high-
591 latitude fringing reef in the GoA from 1994 - 1996 (Dullo et al., 1996), which is methodologically similar to the
592 *ReefBudget* approach. Both reef growth estimates provide similar rates: The TA-based reef accretion estimate from
593 1998 was $0.9 \text{ kg CaCO}_3 \text{ m}^{-2} \text{ y}^{-1}$ and the GoA fringing reef budget from 1994 - 1996 ranged between 0.7 and 0.9 kg
594 $\text{CaCO}_3 \text{ m}^{-2} \text{ y}^{-1}$. Additionally, the gross calcification rate of the offshore benthic communities (G_{benthos}) compares well
595 with the maxima measured in the GoA reefs in 1994 (i.e., $2.7 \text{ kg CaCO}_3 \text{ m}^{-2} \text{ y}^{-1}$) (Heiss, 1995). The G_{budgets} assessed
596 in the present study are in accordance with these data, indicating stable reef growth rates in the Red Sea basin in the
597 recent 20 years, despite the ongoing warming trend and observed impairment in coral calcification in a coral species
598 (Cantin et al., 2010; Raitsois et al., 2011). Yet, data are limited and comparisons between the central Red Sea and the
599 GoA should be interpreted with great caution. Due to the strong latitudinal gradient of temperature and salinity along
600 with differences in seasonality between the central Red Sea and the GoA, reef growth dynamics from the two regions
601 may fundamentally differ. Hence, far larger (and ideally cross-latitude) datasets will be needed to determine more
602 accurately whether a declining calcification capacity of Red Sea corals has already become a basin-scale phenomenon
603 and whether there are species-specific differences. **In this study we have demonstrated that offshore reefs in the central**
604 **Red Sea still maintain a positive carbonate budget, yet can be considered ‘underperforming’ below “optimal reefal**
605 **production” (Vecsei, 2004). In the context of reef growth trajectories, the data presented in this study should serve as**
606 **a valuable contemporary baseline for comparative future studies in the central Red Sea. Importantly, these data were**
607 **collected before the Third Global Bleaching Event, which impacted the region during summers 2015 and 2016**
608 **(Monroe et al., 2018). The present effort therefore will be of great value when assessing potential (long-term) changes**
609 **of Red Sea G_{budgets} following this substantial disturbance.**

610 **5 Conclusions**

611 The Red Sea is a geographic region where coral reefs exist in a naturally high temperature and high salinity
612 environment. Baseline data for reef growth from this region are scarce and particularly valuable as they provide insight
613 into reef functioning under environmental conditions that deviate from the global average for coral reefs. **As such,**
614 **they can provide a potential outlook to future ocean scenarios. Overall, we found net erosion in a near shore reef site,**
615 **about neutral growth in a midshore reef site, and net accretion in an offshore reef site. A comparison of central Red**
616 **Sea reef growth dynamics to other major reef systems revealed important differences and argue for *in situ* studies in**
617 **underexplored major reef regions.** For instance, our study highlights the importance of coralline algae as a reef-
618 building agent and shows that the erosive forces in the Red Sea are not as pronounced (yet) as observed elsewhere.
619 Reef growth on Red Sea offshore reefs is comparable to the majority of reef growth estimates from other geographic
620 regions, which today perform well below what has been considered a ‘healthy reef’ carbonate budget. A first
621 comparison with data from recent years suggests that reef growth rates in the central Red Sea have not decreased
622 substantially over the last two decades, despite potential negative effects of the ongoing warming trend. The absence
623 of comparative long-term data from the region hampers long-term predictions. We therefore advocate additional
624 research to better inform past and future trajectories of reef growth dynamics under consideration of the challenging
625 and unique environmental settings of the Red Sea.

626

627 **Acknowledgements**

628 We thank the Coastal and Marine Resources Lab (CMOR) at King Abdullah University of Science and Technology
629 (KAUST) for logistics and operations at sea (E. Al-Jahdali, A. Al-Jahdali, G. Al-Jahdali, R. Al-Jahdali, H. Al-Jahdali,
630 F. Mallon, P. Müller, and D. Pallett), as well as for the assistance with the deployment of oceanographic instruments
631 (L. Smith, M.D. Pantalita, and S. Mahmoud). We would like to acknowledge field assistance by C. Roder and C.
632 Walcher in setting up the monitoring sites. We thank M. Khalil for providing a map of the study sites. **We thank the**
633 **comments and suggestion from two anonymous reviewers and S. Comeau (Laboratoire d’Océanographie de**
634 **Villefranche) for his critical comments and helpful suggestions to improve the manuscript.** Research reported in this
635 publication was supported by funding to CRV from KAUST.

636

637 **Data availability.**

638 All data are provided in the manuscript and supplement. In addition, physicochemical datasets, reef census, and
639 limestone block assay raw data are available from the Dryad Digital Repository (<http://XXXXXX>) (*will be included*
640 *after review*)

641 The Supplementary material related to this article is available online (*will be included by Copernicus*)

642 **Author contribution**

643 Resources: CRV

644 Project administration: CRV

645 Conceptualization: AR

646 Investigation: AR TR CP
647 Methodology: AR TR CP
648 Formal analysis: AR CP VS
649 Validation: AR CP TR VS CRV
650 Visualization: AR
651 Funding acquisition: CRV
652 Writing - original draft: AR
653 Writing – review & editing: CRV TR CP VS AR
654 Data curation: AR
655
656 **Competing interests**
657 The authors declare that they have no conflict of interest.
658

659 **References**

- 660 Acker, J., Leptoukh, G., Shen, S., Zhu, T. and Kempler, S.: Remotely-sensed chlorophyll a observations of the
661 northern Red Sea indicate seasonal variability and influence of coastal reefs, *J. Mar. Syst.*, 69(3), 191–204,
662 doi:10.1016/j.jmarsys.2005.12.006, 2008.
- 663 Albright, R., Caldeira, L., Hoffelt, J., Kwiatkowski, L., Maclaren, J. K., Mason, B. M., Nebuchina, Y., Ninokawa, A.,
664 Pongratz, J., Ricke, K. L., Rivlin, T., Schneider, K., Sesboüé, M., Shamberger, K., Silverman, J., Wolfe, K., Zhu, K.
665 and Caldeira, K.: Reversal of ocean acidification enhances net coral reef calcification, *Nature*, advance online
666 publication, doi:10.1038/nature17155, 2016.
- 667 Albright, R., Takeshita, Y., Koweek, D. A., Ninokawa, A., Wolfe, K., Rivlin, T., Nebuchina, Y., Young, J. and
668 Caldeira, K.: Carbon dioxide addition to coral reef waters suppresses net community calcification, *Nature*, 555(7697),
669 516–519, doi:10.1038/nature25968, 2018.
- 670 Alwany, M. A., Thaler, E. and Stachowitsch, M.: Parrotfish bioerosion on Egyptian Red Sea reefs, *J. Exp. Mar. Biol.*
671 *Ecol.*, 371(2), 170–176, doi:10.1016/j.jembe.2009.01.019, 2009.
- 672 Anderson, M. J., Gorley, R. N. and Clarke, K. R.: PERMANOVA+ for PRIMER: Guide to software and statistical
673 methods, 2008.
- 674 Andersson, A. J.: A Fundamental Paradigm for Coral Reef Carbonate Sediment Dissolution, *Coral Reef Res.*, 2, 52,
675 doi:10.3389/fmars.2015.00052, 2015.
- 676 Bak, R. P. M.: Sea urchin bioerosion on coral reefs: place in the carbonate budget and relevant variables, *Coral Reefs*,
677 13(2), 99–103, doi:10.1007/BF00300768, 1994.
- 678 Bak, R. P. M., Nieuwland, G. and Meesters, E. H.: Coral Growth Rates Revisited after 31 Years: What is Causing
679 Lower Extension Rates in *Acropora Palmata*?, *Bull. Mar. Sci.*, 84(3), 287–294, 2009.
- 680 Bannerot, S. P. and Bohnsack, J. A.: A stationary visual census technique for quantitatively assessing community
681 structure of coral reef fishes, NOAA. [online] Available from: <http://core.kmi.open.ac.uk/download/pdf/11018492.pdf>
682 (Accessed 1 September 2014), 1986.
- 683 Bates, N. R., Amat, A. and Andersson, A. J.: Feedbacks and responses of coral calcification on the Bermuda reef
684 system to seasonal changes in biological processes and ocean acidification, *Biogeosciences*, 7(8), 2509–2530,
685 doi:10.5194/bg-7-2509-2010, 2010.
- 686 Bellwood, D. R.: Direct estimate of bioerosion by two parrotfish species, *Chlorurus gibbus* and *C. sordidus*, on the
687 Great Barrier Reef, Australia, *Mar. Biol.*, 121(3), 419–429, doi:10.1007/BF00349451, 1995.
- 688 Bellwood, D. R., Hoey, A. S. and Choat, J. H.: Limited functional redundancy in high diversity systems: resilience
689 and ecosystem function on coral reefs, *Ecol. Lett.*, 6(4), 281–285, 2003.
- 690 Boyd, P. and Hutchins, D.: Understanding the responses of ocean biota to a complex matrix of cumulative
691 anthropogenic change, *Mar. Ecol. Prog. Ser.*, 470, 125–135, doi:10.3354/meps10121, 2012.
- 692 Boyd, P. W. and Brown, C. J.: Modes of interactions between environmental drivers and marine biota, *Front. Mar.*
693 *Sci.*, 2, doi:10.3389/fmars.2015.00009, 2015.
- 694 Browne, N. K., Smithers, S. G. and Perry, C. T.: Carbonate and terrigenous sediment budgets for two inshore turbid
695 reefs on the central Great Barrier Reef, *Mar. Geol.*, 346, 101–123, doi:10.1016/j.margeo.2013.08.011, 2013.

696 Bruggemann, J., van Kessel, A., van Rooij, J. and Breeman, A.: Bioerosion and sediment ingestion by the Caribbean
697 parrotfish *Scarus vetula* and *Sparisoma viride*: implications of fish size, feeding mode and habitat use, *Mar. Ecol.*
698 *Prog. Ser.*, 134, 59–71, doi:10.3354/meps134059, 1996.

699 Buddemeier, R. W.: Symbiosis: Making light work of adaptation, *Nature*, 388(6639), 229–230, doi:10.1038/40755,
700 1997.

701 Cai, W.-J., Ma, Y., Hopkinson, B. M., Grotto, A. G., Warner, M. E., Ding, Q., Hu, X., Yuan, X., Schoepf, V., Xu,
702 H., Han, C., Melman, T. F., Hoadley, K. D., Pettay, D. T., Matsui, Y., Baumann, J. H., Levas, S., Ying, Y. and Wang,
703 Y.: Microelectrode characterization of coral daytime interior pH and carbonate chemistry, *Nat. Commun.*, 7, 11144,
704 doi:10.1038/ncomms11144, 2016.

705 Camp, E. F., Nitschke, M. R., Rodolfo-Metalpa, R., Houlbreque, F., Gardner, S. G., Smith, D. J., Zampighi, M. and
706 Suggett, D. J.: Reef-building corals thrive within hot-acidified and deoxygenated waters, *Sci. Rep.*, 7(1), 2434,
707 doi:10.1038/s41598-017-02383-y, 2017.

708 Camp, E. F., Schoepf, V., Mumby, P. J., Hardtke, L. A., Rodolfo-Metalpa, R., Smith, D. J. and Suggett, D. J.: The
709 Future of Coral Reefs Subject to Rapid Climate Change: Lessons from Natural Extreme Environments, *Front. Mar.*
710 *Sci.*, 5, doi:10.3389/fmars.2018.00004, 2018.

711 Cantin, N. E., Cohen, A. L., Karnauskas, K. B., Tarrant, A. M. and McCorkle, D. C.: Ocean Warming Slows Coral
712 Growth in the Central Red Sea, *Science*, 329(5989), 322–325, doi:10.1126/science.1190182, 2010.

713 Carricart-Ganivet, J. P., Cabanillas-Terán, N., Cruz-Ortega, I. and Blanchon, P.: Sensitivity of Calcification to
714 Thermal Stress Varies among Genera of Massive Reef-Building Corals, *PLoS ONE*, 7(3), e32859,
715 doi:10.1371/journal.pone.0032859, 2012.

716 Chazottes, V., Campion-Alsumard, T. L. and Peyrot-Clausade, M.: Bioerosion rates on coral reefs: interactions
717 between macroborers, microborers and grazers (Moorea, French Polynesia), *Palaeogeogr. Palaeoclimatol. Palaeoecol.*,
718 113(2–4), 189–198, doi:10.1016/0031-0182(95)00043-L, 1995.

719 Chazottes, V., Le Campion-Alsumard, T., Peyrot-Clausade, M. and Cuet, P.: The effects of eutrophication-related
720 alterations to coral reef communities on agents and rates of bioerosion (Reunion Island, Indian Ocean), *Coral Reefs*,
721 21(4), 375–390, 2002.

722 Cohen, A. L. and Holcomb, M.: Why corals care about ocean acidification: uncovering the mechanism, *Oceanography*,
723 (22), 118–127, 2009.

724 Cooper, T. F., Death, G., Fabricius, K. E. and Lough, J. M.: Declining coral calcification in massive *Porites* in two
725 nearshore regions of the northern Great Barrier Reef, *Glob. Change Biol.*, 14(3), 529–538, doi:10.1111/j.1365-
726 2486.2007.01520.x, 2008.

727 Couce, E., Ridgwell, A. and Hendy, E. J.: Environmental controls on the global distribution of shallow-water coral
728 reefs, *J. Biogeogr.*, 39(8), 1508–1523, doi:10.1111/j.1365-2699.2012.02706.x, 2012.

729 Cyronak, T., Santos, I. R., McMahon, A. and Eyre, B. D.: Carbon cycling hysteresis in permeable carbonate sands
730 over a diel cycle: Implications for ocean acidification, *Limnol. Oceanogr.*, 58(1), 131–143,
731 doi:10.4319/lo.2013.58.1.0131, 2013.

732 Death, G., Lough, J. M. and Fabricius, K. E.: Declining Coral Calcification on the Great Barrier Reef, *Science*,
733 323(5910), 116–119, doi:10.1126/science.1165283, 2009.

734 Dullo, P. D. W.-C., Gektidis, D. M., Golubic, P. D. S., Heiss, D. G. A., Kampmann, D. B. H., Kiene, D. W., Kroll, D.,
735 Ö. D. K., Kuhrau, D. B. M. L., Radtke, D. G., Reijmer, D. J. G., Reinicke, D. G. B., Schlichter, P. D. D., Schuhmacher,

- 736 P. D. H. and Vogel, K.: Factors controlling holocene reef growth: An interdisciplinary approach, *Facies*, 32(1), 145–
737 188, doi:10.1007/BF02536867, 1995.
- 738 Dullo, W.-C., Reijmer, J., Schuhmacher, H., Eisenhauer, A., Hassan, M. and Heiss, G.: Holocene reef growth and
739 recent carbonate production in the Red Sea, [online] Available from:
740 [https://www.researchgate.net/publication/230751439_Holocene_reef_growth_and_recent_carbonate_production_in](https://www.researchgate.net/publication/230751439_Holocene_reef_growth_and_recent_carbonate_production_in_the_Red_Sea)
741 [_the_Red_Sea](https://www.researchgate.net/publication/230751439_Holocene_reef_growth_and_recent_carbonate_production_in_the_Red_Sea), 1996.
- 742 Eakin, C. M.: A tale of two Enso Events: carbonate budgets and the influence of two warming disturbances and
743 intervening variability, Uva Island, Panama, *Bull. Mar. Sci.*, 69(1), 171–186, 2001.
- 744 Edinger, E. N., Limmon, G. V., Jompa, J., Widjatmoko, W., Heikoop, J. M. and Risk, M. J.: Normal coral growth
745 rates on dying reefs: Are coral growth rates good indicators of reef health?, *Mar. Pollut. Bull.*, 40(5), 404–425, 2000.
- 746 Enochs, I. C.: Ocean acidification enhances the bioerosion of a common coral reef sponge: implications for the
747 persistence of the Florida Reef Tract, *Bull. Mar. Sci.*, 91, 271–290, doi:10.5343/bms.2014.1045, 2015.
- 748 Eyre, B. D., Cyronak, T., Drupp, P., Carlo, E. H. D., Sachs, J. P. and Andersson, A. J.: Coral reefs will transition to
749 net dissolving before end of century, *Science*, 359(6378), 908–911, doi:10.1126/science.aao1118, 2018.
- 750 Ezzat, L., Maguer, J.-F., Grover, R. and Ferrier-Pagès, C.: Limited phosphorus availability is the Achilles heel of
751 tropical reef corals in a warming ocean, *Sci. Rep.*, 6, 31768, doi:10.1038/srep31768, 2016.
- 752 Fabricius, K. E.: Factors Determining the Resilience of Coral Reefs to Eutrophication: A Review and Conceptual
753 Model, in *Coral Reefs: An Ecosystem in Transition*, edited by Z. Dubinsky and N. Stambler, pp. 493–505, Springer
754 Netherlands, Dordrecht. [online] Available from: [http://www.springerlink.com/index/10.1007/978-94-007-0114-](http://www.springerlink.com/index/10.1007/978-94-007-0114-4_28)
755 [4_28](http://www.springerlink.com/index/10.1007/978-94-007-0114-4_28) (Accessed 8 May 2012), 2011.
- 756 Fahmy, M.: Water quality in the Red Sea coastal waters (Egypt): Analysis of spatial and temporal variability, *Chem.*
757 *Ecol.*, 19(1), 67–77, doi:10.1080/0275754031000087074, 2003.
- 758 Fang, J. K. H., Mello-Athayde, M. A., Schönberg, C. H. L., Kline, D. I., Hoegh-Guldberg, O. and Dove, S.: Sponge
759 biomass and bioerosion rates increase under ocean warming and acidification, *Glob. Change Biol.*, 19(12), 3581–
760 3591, doi:10.1111/gcb.12334, 2013.
- 761 Ferrier-Pagès, C., Godinot, C., D’Angelo, C., Wiedenmann, J. and Grover, R.: Phosphorus metabolism of reef
762 organisms with algal symbionts, *Ecol. Monogr.*, 86(3), 262–277, doi:10.1002/ecm.1217, 2016.
- 763 Franco, C., Hepburn, L. A., Smith, D. J., Nimrod, S. and Tucker, A.: A Bayesian Belief Network to assess rate of
764 changes in coral reef ecosystems, *Environ. Model. Softw.*, 80, 132–142, doi:10.1016/j.envsoft.2016.02.029, 2016.
- 765 Glynn, P. W.: Bioerosion and coral-reef growth: a dynamic balance, in *Life and Death of Coral Reefs*, edited by C.
766 Birkeland, pp. 68–94, Chapman and Hall, Ney York, USA., 1997.
- 767 Glynn, P. W. and Manzello, D. P.: Bioerosion and Coral Reef Growth: A Dynamic Balance, in *Coral Reefs in the*
768 *Anthropocene*, edited by C. Birkeland, pp. 67–97, Springer Netherlands., 2015.
- 769 Graham, N. A. J., Wilson, S. K., Carr, P., Hoey, A. S., Jennings, S. and MacNeil, M. A.: Seabirds enhance coral reef
770 productivity and functioning in the absence of invasive rats, *Nature*, 559(7713), 250–253, doi:10.1038/s41586-018-
771 0202-3, 2018.
- 772 Grand, H. M. L. and Fabricius, K. E.: Relationship of internal macrobioeroder densities in living massive *Porites* to
773 turbidity and chlorophyll on the Australian Great Barrier Reef, *Coral Reefs*, 30(1), 97–107, doi:10.1007/s00338-010-
774 0670-x, 2010.

- 775 Grange, J. S., Rybarczyk, H. and Tribollet, A.: The three steps of the carbonate biogenic dissolution process by
776 microborers in coral reefs (New Caledonia), *Environ. Sci. Pollut. Res.*, doi:10.1007/s11356-014-4069-z, 2015.
- 777 Green, A. L. and Bellwood, D. R.: Monitoring functional groups of herbivorous reef fishes as indicators of coral reef
778 resilience: a practical guide for coral reef managers in the Asia Pacific region, International Union for Conservation
779 of Nature, IUCN, Gland, Switzerland. [online] Available from:
780 ftp://ftp.library.noaa.gov/noaa_documents.lib/CoRIS/IUCN_herbivorous_reef-fishes_2009.pdf (Accessed 30
781 September 2017), 2009.
- 782 Heiss, G. A.: Carbonate production by scleractinian corals at Aqaba, Gulf of Aqaba, Red Sea, *Facies*, 33(1), 19–34,
783 doi:10.1007/BF02537443, 1995.
- 784 Heyward, A. J. and Negri, A. P.: Natural inducers for coral larval metamorphosis, *Coral Reefs*, 18(3), 273–279, 1999.
- 785 Hoey, A. S. and Bellwood, D. R.: Cross-shelf variation in the role of parrotfishes on the Great Barrier Reef, *Coral
786 Reefs*, 27(1), 37–47, doi:10.1007/s00338-007-0287-x, 2007.
- 787 Holmes, K. E.: Effects of eutrophication on bioeroding sponge communities with the description of new West Indian
788 sponges, *Cliona* spp. (Porifera: Hadromerida: Clionidae), *Invertebr. Biol.*, 119(2), 125–138, doi:10.1111/j.1744-
789 7410.2000.tb00001.x, 2000.
- 790 Hutchings, P. A.: Biological destruction of coral reefs, *Coral Reefs*, 4(4), 239–252, doi:10.1007/BF00298083, 1986.
- 791 Januchowski-Hartley, F. A., Graham, N. A. J., Wilson, S. K., Jennings, S. and Perry, C. T.: Drivers and predictions
792 of coral reef carbonate budget trajectories, *Proc R Soc B*, 284(1847), 20162533, doi:10.1098/rspb.2016.2533, 2017.
- 793 Jokiel, P. L. and Coles, S. L.: Response of Hawaiian and other Indo-Pacific reef corals to elevated temperature, *Coral
794 Reefs*, 8(4), 155–162, doi:10.1007/BF00265006, 1990.
- 795 Jones, N. S., Ridgwell, A. and Hendy, E. J.: Evaluation of coral reef carbonate production models at a global scale,
796 *Biogeosciences*, 12(5), 1339–1356, doi:10.5194/bg-12-1339-2015, 2015.
- 797 Kattan, A., Coker, D. J. and Berumen, M. L.: Reef fish communities in the central Red Sea show evidence of
798 asymmetrical fishing pressure, *Mar. Biodivers.*, 1–12, doi:10.1007/s12526-017-0665-8, 2017.
- 799 Kennedy, E. V., Perry, C. T., Halloran, P. R., Iglesias-Prieto, R., Schönberg, C. H. L., Wisshak, M., Form, A. U.,
800 Carricart-Ganivet, J. P., Fine, M., Eakin, C. M. and Mumby, P. J.: Avoiding Coral Reef Functional Collapse Requires
801 Local and Global Action, *Curr. Biol.*, 23(10), 912–918, doi:10.1016/j.cub.2013.04.020, 2013.
- 802 Kiene, W. E. and Hutchings, P. A.: Bioerosion experiments at Lizard Island, Great Barrier Reef, *Coral Reefs*, 13(2),
803 91–98, 1994.
- 804 Kleemann, K.: The Pectinid Bivalve *Pedum spondyloideum* (Gmelin 1791): Amount of Surface and Volume Occupied
805 in Host Corals From the Red Sea, *Mar. Ecol.*, 22(1–2), 111–133, doi:10.1046/j.1439-0485.2001.01749.x, 2001.
- 806 Kleypas, J., Buddemeier, R. and Gattuso, J.-P.: The future of coral reefs in an age of global change, *Int. J. Earth Sci.*,
807 90(2), 426–437, doi:10.1007/s005310000125, 2001.
- 808 Kleypas, J. A., McManus, J. W. and Menez, L. A. B.: Environmental Limits to Coral Reef Development: Where Do
809 We Draw the Line?, *Am. Zool.*, 39, 146–159, 1999.
- 810 LaJeunesse, T. C., Parkinson, J. E., Gabrielson, P. W., Jeong, H. J., Reimer, J. D., Voolstra, C. R. and Santos, S. R.:
811 Systematic Revision of Symbiodiniaceae Highlights the Antiquity and Diversity of Coral Endosymbionts, *Curr. Biol.*,
812 28(16), 2570-2580.e6, doi:10.1016/j.cub.2018.07.008, 2018.

- 813 Langdon, C., Takahashi, T., Sweeney, C., Chipman, D., Goddard, J., Marubini, F., Aceves, H., Barnett, H. and
814 Atkinson, M. J.: Effect of calcium carbonate saturation state on the calcification rate of an experimental coral reef,
815 *Glob. Biogeochem. Cycles*, 14(2), 639–654, doi:10.1029/1999GB001195, 2000.
- 816 Lazar, B. and Loya, Y.: Bioerosion of coral reefs - A chemical approach, *Limnol. Oceanogr.*, 36, 377–383, 1991.
- 817 Manzello, D. P.: Ocean acidification hotspots: Spatiotemporal dynamics of the seawater CO₂ system of eastern Pacific
818 coral reefs, *Limnol. Oceanogr.*, 55(1), 239–248, doi:10.4319/lo.2010.55.1.0239, 2010.
- 819 Marshall, A. T. and Clode, P.: Calcification rate and the effect of temperature in a zooxanthellate and an
820 azooxanthellate scleractinian reef coral, *Coral Reefs*, 23(2), 218–224, doi:10.1007/s00338-004-0369-y, 2004.
- 821 Marubini, F., Ferrier-Pagès, C., Furla, P. and Allemand, D.: Coral calcification responds to seawater acidification: a
822 working hypothesis towards a physiological mechanism, *Coral Reefs*, 27(3), 491–499, doi:10.1007/s00338-008-0375-
823 6, 2008.
- 824 McClanahan, T. R.: Kenyan coral reef lagoon fish: effects of fishing, substrate complexity, and sea urchins, *Coral
825 Reefs*, 13(4), 231–241, doi:10.1007/BF00303637, 1994.
- 826 McClanahan, T. R. and Shafir, S. H.: Causes and consequences of sea urchin abundance and diversity in Kenyan coral
827 reef lagoons, *Oecologia*, 83(3), 362–370, doi:10.1007/BF00317561, 1990.
- 828 McClanahan, T. R., Nugues, M. and Mwachireya, S.: Fish and sea urchin herbivory and competition in Kenyan coral
829 reef lagoons: the role of reef management, *J. Exp. Mar. Biol. Ecol.*, 184(2), 237–254, doi:10.1016/0022-
830 0981(94)90007-8, 1994.
- 831 Metzl, N., Moore, B., Papaud, A. and Poisson, A.: Transport and carbon exchanges in Red Sea Inverse Methodology,
832 *Glob. Biogeochem. Cycles*, 3(1), 1–26, doi:10.1029/GB003i001p00001, 1989.
- 833 Moberg, F. and Folke, C.: Ecological goods and services of coral reef ecosystems, *Ecol. Econ.*, 29, 215–233, 1999.
- 834 Mokady, O., Lazar, B. and Loya, Y.: Echinoid bioerosion as a major structuring force of Red Sea coral reefs, *Biol.
835 Bull.*, 190(3), 367–372, 1996.
- 836 Monroe, A. A., Ziegler, M., Roik, A., Röthig, T., Hardenstine, R. S., Emms, M. A., Jensen, T., Voolstra, C. R. and
837 Berumen, M. L.: *In situ* observations of coral bleaching in the central Saudi Arabian Red Sea during the 2015/2016
838 global coral bleaching event, *PLoS ONE*, 13(4), e0195814, doi:10.1371/journal.pone.0195814, 2018.
- 839 Orr, J. C., Fabry, V. J., Aumont, O., Bopp, L., Doney, S. C., Feely, R. A., Gnanadesikan, A., Gruber, N., Ishida, A.,
840 Joos, F., Key, R. M., Lindsay, K., Maier-Reimer, E., Matear, R., Monfray, P., Mouchet, A., Najjar, R. G., Plattner,
841 G.-K., Rodgers, K. B., Sabine, C. L., Sarmiento, J. L., Schlitzer, R., Slater, R. D., Totterdell, I. J., Weirig, M.-F.,
842 Yamanaka, Y. and Yool, A.: Anthropogenic ocean acidification over the twenty-first century and its impact on
843 calcifying organisms, *Nature*, 437(7059), 681–686, doi:10.1038/nature04095, 2005.
- 844 Osman, E. O., Smith, D. J., Ziegler, M., Kürten, B., Conrad, C., El-Haddad, K. M., Voolstra, C. R. and Suggett, D. J.:
845 Thermal refugia against coral bleaching throughout the northern Red Sea, *Glob. Change Biol.*, 24(2), e474–e484,
846 doi:10.1111/gcb.13895, 2018.
- 847 Osorno, A., Peyrot-Clausade, M. and Hutchings, P. A.: Patterns and rates of erosion in dead *Porites* across the Great
848 Barrier Reef (Australia) after 2 years and 4 years of exposure, *Coral Reefs*, 24(2), 292–303, doi:10.1007/s00338-005-
849 0478-2, 2005.
- 850 Pari, N., Peyrot-Clausade, M., Le Champion-Alsumard, T., Hutchings, P., Chazottes, V., Gobulic, S., Le Champion,
851 J. and Fontaine, M. F.: Bioerosion of experimental substrates on high islands and on atoll lagoons (French Polynesia)
852 after two years of exposure, *Mar. Ecol. Prog. Ser.*, 166, 119–130, 1998.

853 Perry, C., Edinger, E., Kench, P., Murphy, G., Smithers, S., Steneck, R. and Mumby, P.: Estimating rates of
854 biologically driven coral reef framework production and erosion: a new census-based carbonate budget methodology
855 and applications to the reefs of Bonaire, *Coral Reefs*, 31(3), 853–868, doi:10.1007/s00338-012-0901-4, 2012.

856 Perry, C. T. and Morgan, K. M.: Bleaching drives collapse in reef carbonate budgets and reef growth potential on
857 southern Maldives reefs, *Sci. Rep.*, 7, 40581, doi:10.1038/srep40581, 2017.

858 Perry, C. T., Spencer, T. and Kench, P. S.: Carbonate budgets and reef production states: a geomorphic perspective
859 on the ecological phase-shift concept, *Coral Reefs*, 27(4), 853–866, doi:10.1007/s00338-008-0418-z, 2008.

860 Perry, C. T., Murphy, G. N., Kench, P. S., Smithers, S. G., Edinger, E. N., Steneck, R. S. and Mumby, P. J.: Caribbean-
861 wide decline in carbonate production threatens coral reef growth, *Nat. Commun.*, 4, 1402, doi:10.1038/ncomms2409,
862 2013.

863 Perry, C. T., Murphy, G. N., Kench, P. S., Edinger, E. N., Smithers, S. G., Steneck, R. S. and Mumby, P. J.: Changing
864 dynamics of Caribbean reef carbonate budgets: emergence of reef bioeroders as critical controls on present and future
865 reef growth potential, *Proc. R. Soc. B Biol. Sci.*, 281(1796), 20142018–20142018, doi:10.1098/rspb.2014.2018, 2014.

866 Perry, C. T., Murphy, G. N., Graham, N. A. J., Wilson, S. K., Januchowski-Hartley, F. A. and East, H. K.: Remote
867 coral reefs can sustain high growth potential and may match future sea-level trends, *Sci. Rep.*, 5, 18289,
868 doi:10.1038/srep18289, 2015.

869 Perry, C. T., Morgan, K. M. and Yarlett, R. T.: Reef Habitat Type and Spatial Extent as Interacting Controls on
870 Platform-Scale Carbonate Budgets, *Front. Mar. Sci.*, 4, doi:10.3389/fmars.2017.00185, 2017.

871 Perry, C. T., Alvarez-Filip, L., Graham, N. A. J., Mumby, P. J., Wilson, S. K., Kench, P. S., Manzello, D. P., Morgan,
872 K. M., Slangen, A. B. A., Thomson, D. P., Januchowski-Hartley, F., Smithers, S. G., Steneck, R. S., Carlton, R.,
873 Edinger, E. N., Enochs, I. C., Estrada-Saldívar, N., Haywood, M. D. E., Kolodziej, G., Murphy, G. N., Pérez-
874 Cervantes, E., Suchley, A., Valentino, L., Boenish, R., Wilson, M. and Macdonald, C.: Loss of coral reef growth
875 capacity to track future increases in sea level, *Nature*, 1, doi:10.1038/s41586-018-0194-z, 2018.

876 Pisapia, C., Burn, D., Yoosuf, R., Najeeb, A., Anderson, K. D. and Pratchett, M. S.: Coral recovery in the central
877 Maldives archipelago since the last major mass-bleaching, in 1998, *Sci. Rep.*, 6, 34720, doi:10.1038/srep34720, 2016.

878 Pogoreutz, C., Rådecker, N., Cárdenas, A., Gärdes, A., Voolstra, C. R. and Wild, C.: Sugar enrichment provides
879 evidence for a role of nitrogen fixation in coral bleaching, *Glob. Change Biol.*, 8, 23:3838–3848,
880 doi:10.1111/gcb.13695, 2017.

881 Price, N. N., Martz, T. R., Brainard, R. E. and Smith, J. E.: Diel Variability in Seawater pH Relates to Calcification
882 and Benthic Community Structure on Coral Reefs, *PLoS ONE*, 7(8), e43843, doi:10.1371/journal.pone.0043843,
883 2012.

884 R Core Team: R: A language and environment for statistical computing, R Foundation for Statistical Computing,
885 Vienna, Austria. [online] Available from: <http://www.R-project.org/>, 2013.

886 Rådecker, N., Pogoreutz, C., Voolstra, C. R., Wiedenmann, J. and Wild, C.: Nitrogen cycling in corals: the key to
887 understanding holobiont functioning?, *Trends Microbiol.*, doi:10.1016/j.tim.2015.03.008, 2015.

888 Raitso, D. E., Hoteit, I., Prihartato, P. K., Chronis, T., Triantafyllou, G. and Abualnaja, Y.: Abrupt warming of the
889 Red Sea, *Geophys. Res. Lett.*, 38(14), L14601, doi:10.1029/2011GL047984, 2011.

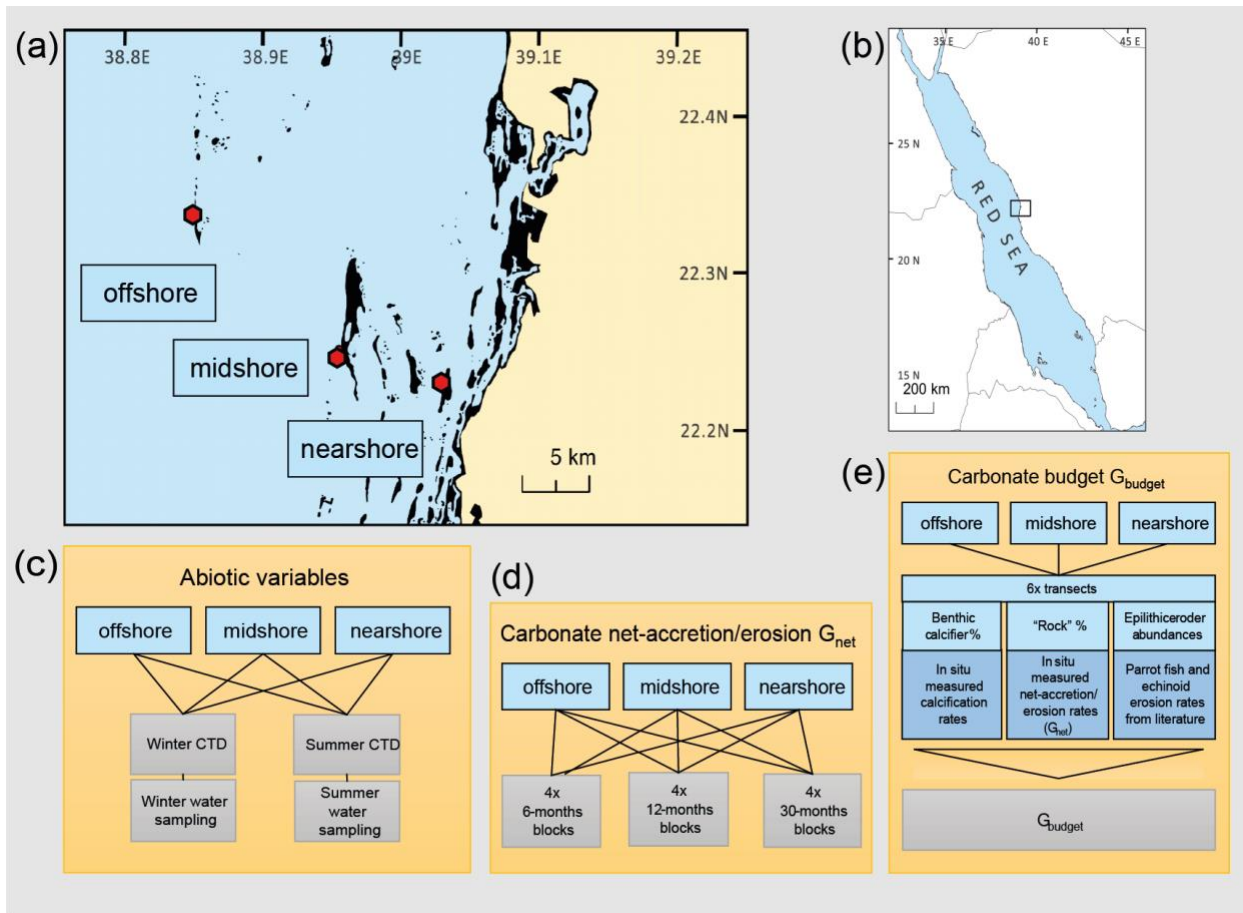
890 Reaka-Kudla, M., Feingold, J. and Glynn, W.: Experimental studies of rapid bioerosion of coral reefs in the Galapagos
891 Islands, *Coral Reefs*, 15(2), 101–107, 1996.

- 892 Reaka-Kudla, M. L.: The Global Biodiversity of Coral Reefs: A Comparison with Rainforests, in Biodiversity II:
893 Understanding and Protecting Our Biological Resources, edited by M. L. Reaka-Kudla, D. E. Wilson, and E. O.
894 Wilson, pp. 83–106, The Joseph Henry Press, USA., 1997.
- 895 Riegl, B.: Climate change and coral reefs: different effects in two high-latitude areas (Arabian Gulf, South Africa),
896 Coral Reefs, 22(4), 433–446, doi:10.1007/s00338-003-0335-0, 2003.
- 897 Riegl, B. M., Bruckner, A. W., Rowlands, G. P., Purkis, S. J. and Renaud, P.: Red Sea Coral Reef Trajectories over 2
898 Decades Suggest Increasing Community Homogenization and Decline in Coral Size, PLoS ONE, 7(5), e38396,
899 doi:10.1371/journal.pone.0038396, 2012.
- 900 Roik, A., Roder, C., Röthig, T. and Voolstra, C. R.: Spatial and seasonal reef calcification in corals and calcareous
901 crusts in the central Red Sea, Coral Reefs, 1–13, doi:10.1007/s00338-015-1383-y, 2015.
- 902 Roik, A., Röthig, T., Roder, C., Ziegler, M., Kremb, S. G. and Voolstra, C. R.: Year-Long Monitoring of Physico-
903 Chemical and Biological Variables Provide a Comparative Baseline of Coral Reef Functioning in the Central Red Sea,
904 PLOS ONE, 11(11), e0163939, doi:10.1371/journal.pone.0163939, 2016.
- 905 Röthig, T., Ochsenkühn, M. A., Roik, A., van der Merwe, R. and Voolstra, C. R.: Long-term salinity tolerance is
906 accompanied by major restructuring of the coral bacterial microbiome, Mol. Ecol., 25(6), 1308–1323,
907 doi:10.1111/mec.13567, 2016.
- 908 Sawall, Y. and Al-Sofyani, A.: Biology of Red Sea Corals: Metabolism, Reproduction, Acclimatization, and
909 Adaptation, in The Red Sea, edited by N. M. A. Rasul and I. C. F. Stewart, pp. 487–509, Springer Berlin Heidelberg.
910 [online] Available from: http://link.springer.com/chapter/10.1007/978-3-662-45201-1_28 (Accessed 7 April 2015),
911 2015.
- 912 Sawall, Y., Al-Sofyani, A., Hohn, S., Banguera-Hinestroza, E., Voolstra, C. R. and Wahl, M.: Extensive phenotypic
913 plasticity of a Red Sea coral over a strong latitudinal temperature gradient suggests limited acclimatization potential
914 to warming, Sci. Rep., 5, 8940, doi:10.1038/srep08940, 2015.
- 915 Schmidt, G. M. and Richter, C.: Coral Growth and Bioerosion of *Porites lutea* in Response to Large Amplitude
916 Internal Waves, PLoS ONE, 8(12), e73236, doi:10.1371/journal.pone.0073236, 2013.
- 917 Schneider, K. and Erez, J.: The effect of carbonate chemistry on calcification and photosynthesis in the hermatypic
918 coral *Acropora eurystroma*, Limnol. Oceanogr., 51(3), 1284–1293, 2006.
- 919 Schönberg, C. H. L., Fang, J. K. H., Carreiro-Silva, M., Tribollet, A. and Wisshak, M.: Bioerosion: the other ocean
920 acidification problem, ICES J. Mar. Sci., 74(4), 895–925, doi:10.1093/icesjms/fsw254, 2017.
- 921 Schuhmacher, H., Loch, K., Loch, W. and See, W. R.: The aftermath of coral bleaching on a Maldivian reef—a
922 quantitative study, Facies, 51(1–4), 80–92, doi:10.1007/s10347-005-0020-6, 2005.
- 923 Shamberger, K. E. F., Lentz, S. J. and Cohen, A. L.: Low and variable ecosystem calcification in a coral reef lagoon
924 under natural acidification, Limnol. Oceanogr., doi:10.1002/lno.10662, 2017.
- 925 Shaw, E. C., McNeil, B. I. and Tilbrook, B.: Impacts of ocean acidification in naturally variable coral reef flat
926 ecosystems, J. Geophys. Res. Oceans, 117(C03038), doi:10.1029/2011JC007655, 2012.
- 927 Sheppard, C. and Loughland, R.: Coral mortality and recovery in response to increasing temperature in the southern
928 Arabian Gulf, Aquat. Ecosyst. Health Manag., 5(4), 395–402, doi:10.1080/14634980290002020, 2002.
- 929 Silbiger, N. J., Guadayol, O., Thomas, F. I. M. and Donahue, M. J.: Reefs shift from net accretion to net erosion along
930 a natural environmental gradient, Mar. Ecol. Prog. Ser., 515, 33–44, doi:10.3354/meps10999, 2014.

- 931 Silverman, J., Lazar, B. and Erez, J.: Community metabolism of a coral reef exposed to naturally varying dissolved
932 inorganic nutrient loads, *Biogeochemistry*, 84(1), 67–82, doi:10.1007/s10533-007-9075-5, 2007.
- 933 Steiner, Z., Erez, J., Shemesh, A., Yam, R., Katz, A. and Lazar, B.: Basin-scale estimates of pelagic and coral reef
934 calcification in the Red Sea and Western Indian Ocean, *Proc. Natl. Acad. Sci.*, 1414323111,
935 doi:10.1073/pnas.1414323111, 2014.
- 936 Steiner, Z., Turchyn, A. V., Harpaz, E. and Silverman, J.: Water chemistry reveals a significant decline in coral
937 calcification rates in the southern Red Sea, *Nat. Commun.*, 9(1), 3615, doi:10.1038/s41467-018-06030-6, 2018.
- 938 Strahl, J., Stolz, I., Uthicke, S., Vogel, N., Noonan, S. H. C. and Fabricius, K. E.: Physiological and ecological
939 performance differs in four coral taxa at a volcanic carbon dioxide seep, *Comp. Biochem. Physiol. A. Mol. Integr.*
940 *Physiol.*, 184, 179–186, doi:10.1016/j.cbpa.2015.02.018, 2015.
- 941 Tambutté, S., Holcomb, M., Ferrier-Pagès, C., Reynaud, S., Tambutté, É., Zoccola, D. and Allemand, D.: Coral
942 biomineralization: From the gene to the environment, *J. Exp. Mar. Biol. Ecol.*, 408(1–2), 58–78,
943 doi:10.1016/j.jembe.2011.07.026, 2011.
- 944 Tribollet, A. and Golubic, S.: Cross-shelf differences in the pattern and pace of bioerosion of experimental carbonate
945 substrates exposed for 3 years on the northern Great Barrier Reef, Australia, *Coral Reefs*, 24(3), 422–434,
946 doi:10.1007/s00338-005-0003-7, 2005.
- 947 Tribollet, A. and Golubic, S.: Reef Bioerosion: Agents and Processes, in *Coral Reefs: An Ecosystem in Transition*,
948 edited by Z. Dubinsky and N. Stambler, pp. 435–449, Springer Netherlands, Dordrecht. [online] Available from:
949 http://www.springerlink.com/index/10.1007/978-94-007-0114-4_25 (Accessed 7 August 2012), 2011.
- 950 Tribollet, A., Decherf, G., Hutchings, P. and Peyrot-Clausade, M.: Large-scale spatial variability in bioerosion of
951 experimental coral substrates on the Great Barrier Reef (Australia): importance of microborers, *Coral Reefs*, 21(4),
952 424–432, doi:10.1007/s00338-002-0267-0, 2002.
- 953 Tribollet, A., Godinot, C., Atkinson, M. and Langdon, C.: Effects of elevated pCO₂ on dissolution of coral carbonates
954 by microbial euendoliths, *Glob. Biogeochem. Cycles*, 23(3), doi:10.1029/2008GB003286, 2009.
- 955 Uthicke, S., Doyle, J., Duggan, S., Yasuda, N. and McKinnon, A. D.: Outbreak of coral-eating Crown-of-Thorns
956 creates continuous cloud of larvae over 320 km of the Great Barrier Reef, *Sci. Rep.*, 5, doi:10.1038/srep16885, 2015.
- 957 Vásquez-Elizondo, R. M. and Enríquez, S.: Coralline algal physiology is more adversely affected by elevated
958 temperature than reduced pH, *Sci. Rep.*, 6, 19030, doi:10.1038/srep19030, 2016.
- 959 Vecsei, A.: Fore-reef carbonate production: development of a regional census-based method and first estimates,
960 *Palaeogeogr. Palaeoclimatol. Palaeoecol.*, 175(1–4), 185–200, doi:10.1016/S0031-0182(01)00371-6, 2001.
- 961 Vecsei, A.: A new estimate of global reefal carbonate production including the fore-reefs, *Glob. Planet. Change*, 43(1–
962 2), 1–18, doi:10.1016/j.gloplacha.2003.12.002, 2004.
- 963 Waldbusser, G. G., Hales, B. and Haley, B. A.: Calcium carbonate saturation state: on myths and this or that stories,
964 *ICES J. Mar. Sci. J. Cons.*, 73(3), 563–568, doi:10.1093/icesjms/fsv174, 2016.
- 965 Wickham, H. and Chang, W.: ggplot2: An Implementation of the Grammar of Graphics. [online] Available from:
966 <http://cran.r-project.org/web/packages/ggplot2/index.html> (Accessed 25 June 2015), 2015.
- 967 Wiedenmann, J., D'Angelo, C., Smith, E. G., Hunt, A. N., Legiret, F.-E., Postle, A. D. and Achterberg, E. P.: Nutrient
968 enrichment can increase the susceptibility of reef corals to bleaching, *Nat. Clim. Change*, 3(2), 160–164,
969 doi:10.1038/nclimate1661, 2013.

970 Zundevich, A., Lazar, B. and Ilan, M.: Chemical versus mechanical bioerosion of coral reefs by boring sponges -
971 lessons from *Pione cf. vastifica*, J. Exp. Biol., 210(1), 91–96, doi:10.1242/jeb.02627, 2007.

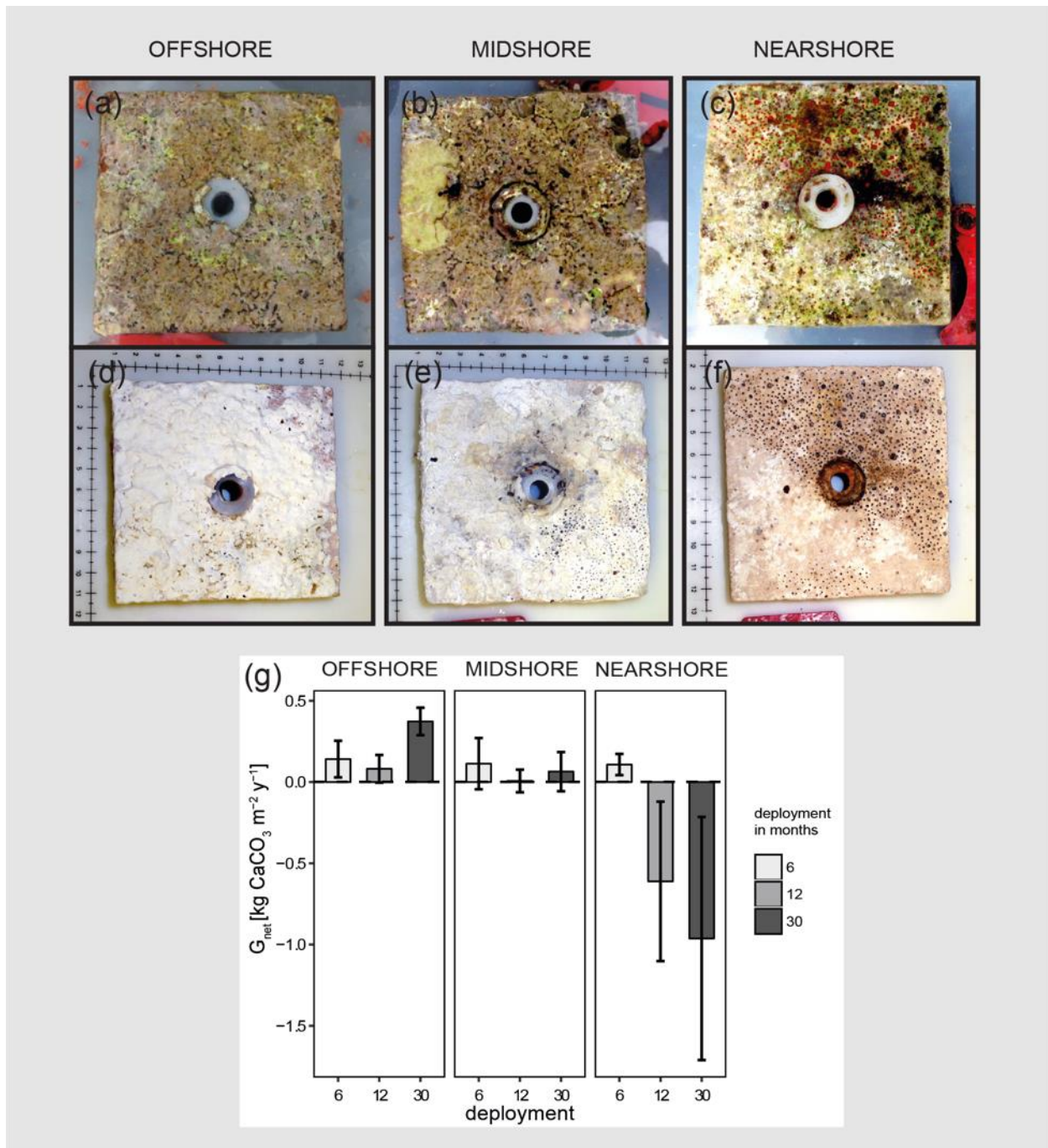
972



974

975 **Figure 1. Design of studies and reef sites in the central Red Sea.** Maps (a) and (b) indicate geographic location and
 976 the study sites along a cross-shelf gradient. Schemes in (c) – (e) summarize the study designs for the assessment of
 977 the two reef growth metrics, G_{net} and G_{budget} , and the characterization of the abiotic environments in the central Red
 978 Sea. Maps have been adapted from Roik et al. (2015).

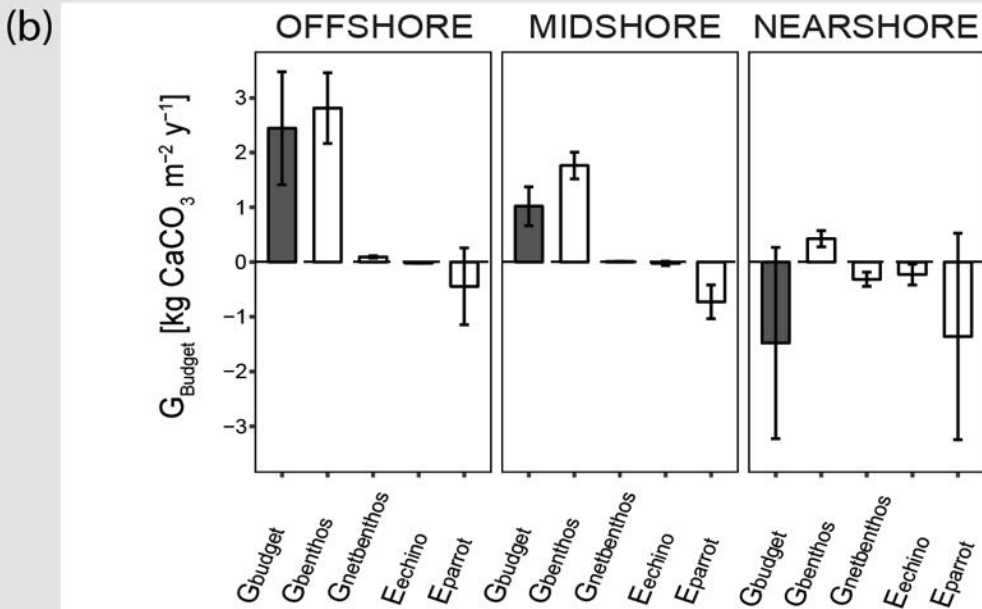
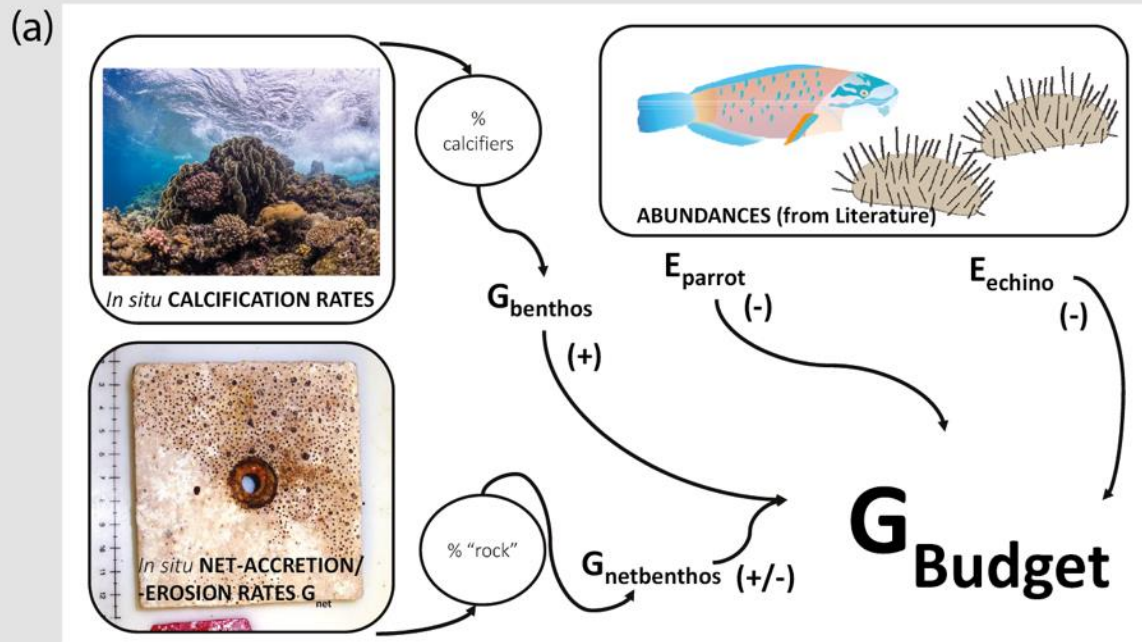
979



980

981 **Figure 2. Net-accretion/erosion rates (G_{net}) in the central Red Sea.** G_{net} were measured *in situ* using limestone
 982 blocks (100 x 100 mm) that were deployed along the cross-shelf gradient, three sets of blocks were deployed for 6,
 983 12, or 30 months, respectively. Photos (a), (b), and (c), show freshly collected limestone blocks that were recovered
 984 after 30 months deployment. The photos (d), (e), and (f) show the same blocks after bleaching and drying. Boring
 985 holes of endolithic sponges are clearly visible in blocks from the nearshore and midshore reef sites. Blocks from the
 986 midshore and offshore reefs are covered with crusts of biogenic carbonate mostly accreted by coralline algae
 987 assemblages (scales in the photos show cm). G_{net} data obtained from the limestone block assay are plotted in (g). All
 988 data are presented as mean \pm standard deviation.

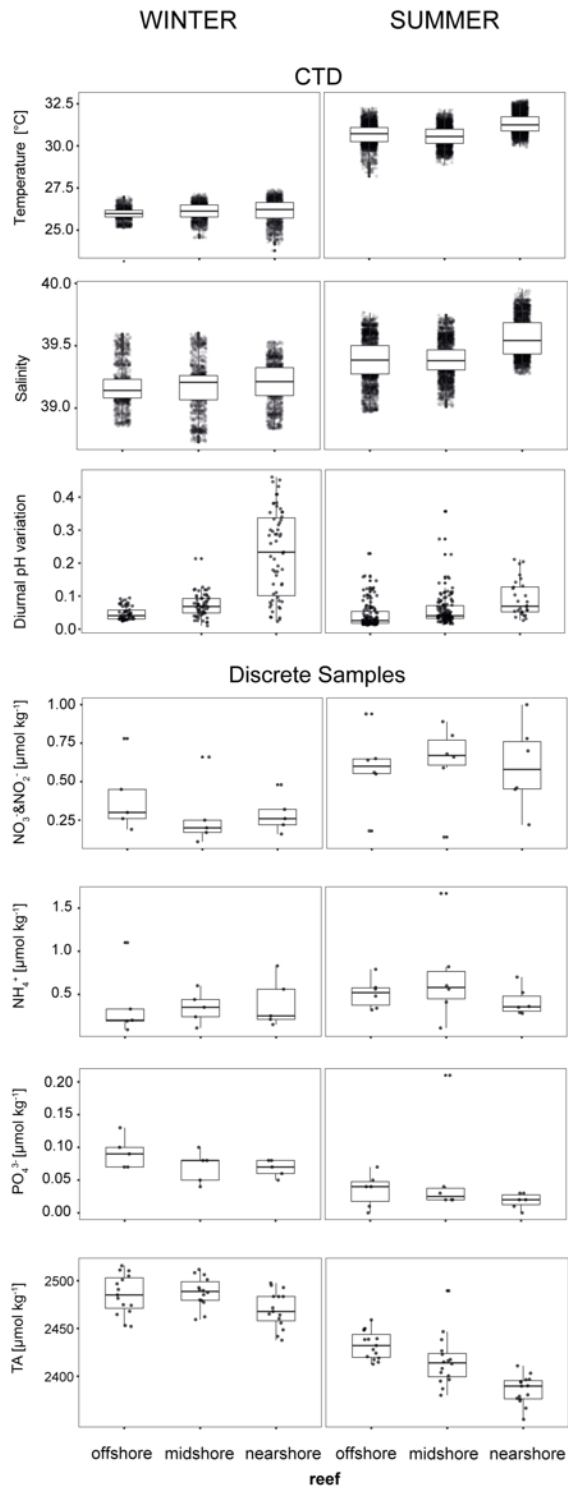
989



990

991 **Figure 3. Census-based carbonate budgets in the central Red Sea.** A schematic overview of the census-based
 992 carbonate budget approach that was adapted from the *ReefBudget* methodology by Perry et al., (2012) is displayed in
 993 (a). Details on input data and equations, employed in the calculations, are available as Supplementary Materials (Text
 994 S1 and respective Supplemental Tables). In (b) reef carbonate budgets are plotted in dark grey (G_{budget}) and related
 995 biotic variables in white. The biotic variables, i.e., site-specific calcification rates of benthic communities (G_{benthos}),
 996 net-accretion/-erosion rates of reef "rock" surface area ($G_{\text{netbenthos}}$), and the epilithic erosion rates of echinoids and
 997 parrotfishes (E_{echino} , E_{parrot}) contribute to the total reef carbonate budget (G_{budget}) at each reef site. All data are presented
 998 as mean \pm standard deviation. Images from www.ian.umces.edu; photos by A.Roik.

999



1000

1001 **Figure 4. Abiotic conditions in the reef sites.** Temperature, salinity, and diurnal pH_{NBS} variation (= diurnal standard
 1002 deviations) were measured continuously over the respective seasons by CTDs (conductivity-temperature-depth
 1003 loggers including an auxiliary pH probe). Furthermore, inorganic nutrients and total alkalinity (TA) were measured in
 1004 discrete samples across reef sites and seasons. Boxplots illustrate the differences of seawater parameters between the
 1005 reefs within each season (box: 1st and 3rd quartiles, whiskers: 1.5-fold inter-quartile range, points: raw data scatter).

1006 **Tables**

1007 **Table 1. Glossary of reef growth metrics.**

Metric	Description	Input data for calculation of the metric
G_{net}	Site-specific net-accretion/-erosion rates (internal and epilithic) measured <i>in situ</i> using limestone blocks	-
* G_{budget}	Ecosystem-scale census-based carbonate budget of a reef site	$G_{benthos}$, $G_{netbenthos}$, $G_{netbenthos}$, E_{echino} , E_{parrot}
$G_{benthos}$	Census-based calcification rate of benthic calcifier community (corals and coralline algae) per reef site	Site-specific benthic calcification rates (collated from this study and from Roik et al. 2015)
$G_{netbenthos}$	Census-based net-accretion/-erosion rates of reef “rock” surface area per reef site	Site-specific net-accretion/-erosion rates measured in this study using limestone blocks (G_{net})
E_{echino}	Census-based echinoid (sea urchin) erosion rates per reef site	Genus and size specific erosion rates for sea urchins from literature
E_{parrot}	Census-based parrotfish erosion rate per reef site	Genus and size specific erosion rates for parrotfishes from literature

*The method of G_{budget} calculation is described in the supplements (please refer to Text S1).

1008
1009
1010

1011 **Table 2. Net-accretion/-erosion rates G_{net} [kg CaCO₃ m⁻² y⁻¹] in coral reefs along a cross-shelf gradient in the central Red**
 1012 **Sea.** G_{net} was calculated using weight gain/loss of limestone blocks that were deployed in the reefs. For each deployment duration,
 1013 6, 12, and 30 months, a set of 4 replicate blocks was used. Each block was measured once. Provided are means per reef site and
 1014 standard deviations (in brackets).

G_{net}	Deployment time [months]		
	6	12	30
Reef site			
Offshore	0.14(0.11)	0.08(0.09)	0.37(0.08)
Midshore	0.11(0.16)	0.01(0.07)	0.06(0.12)
Nearshore	0.11(0.07)	-0.61(0.49)	-0.96(0.75)

1015

1016

1017 **Table 3. Reef carbonate budgets and contributing biotic variables [kg CaCO₃ m⁻² y⁻¹] along a cross-shelf gradient in the**
 1018 **central Red Sea.** Calcification rates of benthic calcifiers (G_{benthos}), net-accretion/-erosion rates of the reef “rock” surface area
 1019 ($G_{\text{netbenthos}}$), and the erosion rates of echinoids and parrotfishes (E_{echino} , E_{parrot}) contribute to the total carbonate budget (G_{budget}) at a
 1020 reef site. Shown are means per site are shown and standard deviations (in brackets).

Reef	G_{budget}	G_{benthos}	$G_{\text{netbenthos}}$	E_{echino}	E_{parrot}
Offshore	2.44(1.03)	2.81(0.65)	0.09(0.02)	-0.02(0)	-0.44(0.7)
Midshore	1.02(0.35)	1.76(0.24)	0.01(0)	-0.02(0.04)	-0.73(0.31)
Nearshore	-1.48(1.75)	0.43(0.15)	-0.31(0.13)	-0.23(0.19)	-1.36(1.89)

1021

1022 **Table 4. Abiotic parameters relevant for reef growth at the study sites along a cross-shelf gradient in the central Red Sea.**
 1023 Temperature (Temp), salinity (Sal), and diurnal pH variation (diurnal SDs of pH_{NBS} measurements) were continuously measured
 1024 using *in situ* probes (CTDs). Weekly collected seawater samples were used for the determination of inorganic nutrient
 1025 concentrations, i.e. nitrate and nitrite (NO₃⁻ & NO₂⁻), ammonia (NH₄⁺), phosphate (PO₄³⁻), and total alkalinity (TA). Provided are
 1026 means and standard deviations (in brackets).

Site / Season	Temp [°C]	Sal	Diurnal pH variation	NO ₃ ⁻ & NO ₂ ⁻ [μmol kg ⁻¹]	NH ₄ ⁺ [μmol kg ⁻¹]	PO ₄ ³⁻ [μmol kg ⁻¹]	TA [μmol kg ⁻¹]
Avg. winter	26.07(0.54)	39.18(0.18)	0.11(0.12)	0.32(0.19)	0.38(0.29)	0.08(0.02)	2487(20)
Avg. summer	30.85(0.69)	39.44(0.18)	0.05(0.05)	0.61(0.25)	0.54(0.34)	0.04(0.05)	2417(27)
Offshore / winter	25.97(0.36)	39.18(0.16)	0.04(0.02)	0.4(0.23)	0.38(0.41)	0.09(0.02)	2492(21)
Offshore / summer	30.68(0.63)	39.38(0.17)	0.04(0.04)	0.59(0.24)	0.51(0.17)	0.04(0.03)	2439(15)
Midshore / winter	26.1(0.49)	39.17(0.2)	0.07(0.04)	0.28(0.22)	0.35(0.19)	0.07(0.02)	2494(16)
Midshore / summer	30.56(0.61)	39.39(0.14)	0.05(0.05)	0.63(0.26)	0.7(0.53)	0.06(0.08)	2422(26)
Nearshore / winter	26.13(0.69)	39.2(0.17)	0.23(0.14)	0.29(0.12)	0.4(0.29)	0.07(0.01)	2476(19)
Nearshore / summer	31.32(0.59)	39.56(0.15)	0.09(0.06)	0.6(0.28)	0.42(0.16)	0.02(0.01)	2391(15)

1027

1028

1029 **Table 5. Coefficients from Spearman rank order correlations for abiotic and biotic predictor variables vs. G_{net} and G_{budget} .**
 1030 The means of abiotic and biotic variables per reef site were correlated with G_{net} (= net-accretion/-erosion rates of limestone blocks)
 1031 and G_{budget} (= census-based carbonate budgets). Strong and significant correlations (ρ values > |0.75|) are marked in **bold**. P -values
 1032 were adjusted by the Benjamini-Hochberg method. CCA = crustose coralline algae; CC = calcifying crusts

Abiotic variables	G_{net}		G_{budget}	
	ρ	$p(adj.)$	ρ	$p(adj.)$
Temperature	-0.47	<i>n.s.</i>	-0.52	<i>n.s.</i>
Salinity	-0.82	< 0.01	-0.82	0.001
Diurnal pH variation	-0.95	< 0.001	-0.89	< 0.001
NO ₃ ⁻ &NO ₂ ⁻	0.95	< 0.001	0.89	< 0.001
NH ₄ ⁺	0.47	<i>n.s.</i>	0.52	<i>n.s.</i>
PO ₄ ³⁻	0.82	< 0.01	0.82	0.001
TA	0.95	< 0.001	0.89	< 0.001
Biotic variables	ρ	$p(adj.)$	ρ	$p(adj.)$
% cover CCA/CC	0.95	< 0.001	0.78	< 0.01
% cover Algae/Soft coral/Sponge	0.47	<i>n.s.</i>	0.26	<i>n.s.</i>
Parrot fish abundance	-0.95	< 0.001	-0.49	<i>n.s.</i>
Echinoid abundance	0.47	<i>n.s.</i>	-0.54	<i>n.s.</i>
% cover branching hard corals			-0.25	<i>n.s.</i>
% cover encrusting hard corals			0.26	<i>n.s.</i>
% cover massive hard corals			0.34	<i>n.s.</i>
% cover foliose hard corals			0.50	<i>n.s.</i>
% cover Acroporidae			0.27	<i>n.s.</i>
% cover Pocilloporidae			0.51	<i>n.s.</i>
% cover Poritidae			0.45	<i>n.s.</i>
% cover hard coral			0.63	<i>n.s.</i>
Rugosity			0.75	< 0.01

1033